A Genome-Wide Screen Reveals a Role for the HIR Histone Chaperone Complex in Preventing Mislocalization of Budding Yeast CENP-A

Sultan Ciftci-Yilmaz,*,[1,2] Wei-Chun Au,*,[1] Prashant K. Mishra,*,[1] Jessica R. Eisenstatt,* Joy Chang,* Anthony R. Dawson,* Iris Zhu,† Mahfuzur Rahman,‡ Sven Bilke,* Michael Costanzo,§ Anastasia Baryshnikova,,[3] Chad L. Myers,‡ Paul S. Meltzer,* David Landsman,† Richard E. Baker,†† Charles Boone,§ and Munira A. Basrai*,[4]**

*Genetics Branch, Center for Cancer Research, National Cancer Institute and †National Center for Biotechnology Information, National Library of Medicine, National Institutes of Health, Bethesda, Maryland 20894, ‡Department of Computer Science and Engineering, University of Minnesota-Twin Cities, Minneapolis, Minnesota 55455, §Donnelly Centre for Cellular and Biomolecular Research, University of Toronto, Ontario M5S 3E1, Canada, **Lewis-Sigler Institute for Integrative Genomics, Princeton University, New Jersey 08544, and ††Department of Microbiology and Physiological Systems, University of Massachusetts Medical School, Worcester, Massachusetts 01655

ORCID ID: 0000-0002-1026-5972 (C.L.M.)

ABSTRACT Centromeric localization of the evolutionarily conserved centromere-specific histone H3 variant CENP-A (Cse4 in yeast) is essential for faithful chromosome segregation. Overexpression and mislocalization of CENP-A lead to chromosome segregation defects in yeast, flies, and human cells. Overexpression of CENP-A has been observed in human cancers; however, the molecular mechanisms preventing CENP-A mislocalization are not fully understood. Here, we used a genome-wide synthetic genetic array (SGA) to identify gene deletions that exhibit synthetic dosage lethality (SDL) when Cse4 is overexpressed. Deletion for genes encoding the replication-independent histone chaperone HIR complex (*HIR1*, *HIR2*, *HIR3*, *HPC2*) and a Cse4-specific E3 ubiquitin ligase, *PSH1*, showed highest SDL. We defined a role for Hir2 in proteolysis of Cse4 that prevents mislocalization of Cse4 to noncentromeric regions for genome stability. Hir2 interacts with Cse4 *in vivo*, and *hir2Δ* strains exhibit defects in Cse4 proteolysis and stabilization of chromatin-bound Cse4. Mislocalization of Cse4 to noncentromeric regions with a preferential enrichment at promoter regions was observed in *hir2Δ* strains. We determined that Hir2 facilitates the interaction of Cse4 with Psh1, and that defects in Psh1-mediated proteolysis contribute to increased Cse4 stability and mislocalization of Cse4 in the *hir2Δ* strain. In summary, our genome-wide screen provides insights into pathways that regulate proteolysis of Cse4 and defines a novel role for the HIR complex in preventing mislocalization of Cse4 by facilitating proteolysis of Cse4, thereby promoting genome stability.

KEYWORDS centromere; kinetochore; gene regulation; chromosome segregation; Cse4; CENP-A; histones; histone chaperone

KINETOCHORES (centromeric DNA and associated proteins) serve as an attachment site for microtubules to promote faithful chromosome segregation during mitosis (Allshire and Karpen 2008; Verdaasdonk and Bloom 2011; Burrack and Berman 2012; Choy *et al.* 2012; Maddox *et al.* 2012; McKinley and Cheeseman 2016). The "point centromeres" of budding yeast contain ~125 bp of unique DNA sequences as opposed to "regional centromeres" in other eukaryotes, which are comprised of up to several mega-base pairs of repeated DNA sequences, species-specific satellite DNA arrays, or retrotransposon-derived sequences (Clarke and Carbon 1980; Allshire and Karpen 2008; Verdaasdonk and Bloom 2011; Burrack and Berman 2012; Maddox *et al.* 2012; McKinley and Cheeseman 2016). Despite the divergence

doi: https://doi.org/10.1534/genetics.118.301305
Manuscript received May 21, 2018; accepted for publication July 12, 2018; published Early Online July 16, 2018.
Supplemental material available at Figshare: https://doi.org/10.25386/genetics.6709553.
[1]These authors contributed equally to this work.
[2]Present address: Department of Medicine and Arizona Health Sciences Center, University of Arizona, Tucson, AZ 85719.
[3]Present address: Calico Life Sciences, South San Francisco, CA 94080.
[4]Corresponding author: Genetics Branch, National Cancer Institute, National Institutes of Health, 41 Medlars Dr., Rm. B900, Bethesda, MD 20892. E-mail: basraim@mail.nih.gov

of centromeric DNA sequences, the centromere-specific histone H3 variant (Cse4 in *Saccharomyces cerevisiae*, Cnp1 in *Schizosaccharomyces pombe*, CID in *Drosophila*, and CENP-A in mammals) is evolutionarily conserved from yeast to humans (Przewloka and Glover 2009; Choy *et al.* 2012; Henikoff 2012). Cse4 and its homologs are essential for high-fidelity chromosome segregation (Allshire and Karpen 2008; Verdaasdonk and Bloom 2011; Burrack and Berman 2012; Maddox *et al.* 2012; McKinley and Cheeseman 2016), and Cse4 can functionally replace CENP-A in mammalian cells (Wieland *et al.* 2004).

Overexpression and mislocalization of CENP-A have been observed in many cancers (Tomonaga *et al.* 2003; Amato *et al.* 2009; Hu *et al.* 2010; Y. Li *et al.* 2011; Wu *et al.* 2012; Lacoste *et al.* 2014; Athwal *et al.* 2015); however, the molecular mechanisms associated with this observation are not fully understood. We have recently shown that overexpression of CENP-A leads to its mislocalization to noncentromeric regions and contributes to chromosome instability (CIN) in human cells (Shrestha *et al.* 2017). Mislocalization of CID causes the formation of ectopic kinetochores and leads to mitotic delay, anaphase bridges, chromosome fragmentation, aneuploidy, and lethality in flies (Heun *et al.* 2006). Overexpression of Cnp1 leads to noncentromeric mislocalization, growth and chromosome segregation defects during mitosis and meiosis in fission yeast (Choi *et al.* 2012; Castillo *et al.* 2013; Gonzalez *et al.* 2014). We have previously shown that mislocalization of overexpressed cse4^{16KR}, in which all lysines (K) are mutated to arginine (R) (Collins *et al.* 2004), results in chromosome segregation defects in budding yeast (Au *et al.* 2008). The extent of mislocalization of cse4^{16KR} and CENP-A correlate with the level of chromosome loss in yeast and human cells, respectively (Au *et al.* 2008; Shrestha *et al.* 2017).

Post-translational modifications (PTMs), such as ubiquitination, regulate the cellular levels of Cse4 and its homologs, and prevent its mislocalization to euchromatic regions (Deyter *et al.* 2017). In flies, proteolysis of CID prevents mislocalization to noncentromeric regions (Heun *et al.* 2006; Moreno-Moreno *et al.* 2011). Similar results are observed in fission yeast, where ubiquitin-mediated proteolysis of Cnp1 prevents mislocalization to noncentromeric regions (Gonzalez *et al.* 2014). Additionally, Psh1 (an E3 ubiquitin ligase) (Hewawasam *et al.* 2010; Ranjitkar *et al.* 2010; Herrero and Thorpe 2016; Hildebrand and Biggins 2016), Doa1 (WD-repeat protein) (Au *et al.* 2013), Fpr3 (proline isomerase) (Ohkuni *et al.* 2014), Ubp8 (ubiquitin protease) (Canzonetta *et al.* 2015), Rcy1 (F-box protein) (Cheng *et al.* 2016), and Ubr1 (Cheng *et al.* 2017) regulate cellular levels of overexpressed Cse4 and prevent its mislocalization to noncentromeric regions (Collins *et al.* 2005; Cheng *et al.* 2016). The role of Psh1 in proteolysis of Cse4 has been characterized in detail, and these studies have shown that the interactions of Psh1 with Spt16, a component of the FACT (facilitates chromatin transcription/transactions) complex, and casein kinase 2 (CKA2) regulate Cse4 proteolysis (Hewawasam *et al.* 2010, 2014; Ranjitkar *et al.* 2010; Au *et al.* 2013; Deyter and Biggins 2014). Recent studies have shown that chromatin assembly factor-1 (CAF-1) promotes the deposition of Cse4 at noncentromeric regions in *psh1Δ* mutants, and deletion of Cac2, a component of CAF-1, rescues the lethality of *psh1Δ* or *cka2Δ* strains overexpressing Cse4 (Hewawasam *et al.* 2018). While the centromere-targeting domain (CATD) in the C-terminus of Cse4 interacts with Psh1, the N-terminus of Cse4 is also required for Cse4 proteolysis (Hewawasam *et al.* 2010; Ranjitkar *et al.* 2010; Au *et al.* 2013). In addition to ubiquitination, sumolylation of Cse4 also regulates its proteolysis. We have shown that Cse4 is sumoylated by the small ubiquitin-related modifier (SUMO) E3 ligases Siz1 and Siz2, and the SUMO-targeted ubiquitin ligase (STUbL) Slx5 plays a critical role in ubiquitin-mediated proteolysis of endogenously expressed Cse4 and prevents its mislocalization independently of Psh1 (Ohkuni *et al.* 2016). Notably, overexpressed Cse4 is not completely stabilized in *psh1Δ*, *doa1Δ*, *fpr3Δ*, *rcy1Δ*, and *slx5Δ* strains (Hewawasam *et al.* 2010; Ranjitkar *et al.* 2010; Au *et al.* 2013; Ohkuni *et al.* 2014, 2016; Cheng *et al.* 2016; Hildebrand and Biggins 2016) suggesting the existence of additional genes/pathways to regulate Cse4 proteolysis.

Identification of pathways that regulate cellular levels of Cse4 is critical for understanding mechanisms that prevent mislocalization of CENP-A and aneuploidy in human cancers. Hence, we performed a genome-wide screen using a synthetic genetic array (SGA) to identify nonessential genes that show synthetic dosage lethality (SDL) upon Cse4 overexpression. We hypothesized that overexpression of Cse4 would cause SDL in mutants that are defective in Cse4 proteolysis, similar to that observed previously for *psh1Δ* strains (Ranjitkar *et al.* 2010; Au *et al.* 2013). We identified deletions of all four components of the replication-independent histone chaperone (HIR) complex (*HIR1*, *HIR2*, *HIR3*, *HPC2*) in the screen, and growth assays confirmed the SDL of overexpressed Cse4 in deletion strains for each component of the HIR complex. We investigated the molecular role of Hir2 in Cse4 proteolysis and how this affects the localization of Cse4. Hir2 interacts with Cse4 *in vivo*, and deletion of *HIR2* leads to defects in Cse4 proteolysis and mislocalization of Cse4 to noncentromeric regions. We determined that defects in Psh1-mediated proteolysis of Cse4 contribute to the increased stability of Cse4 in the *hir2Δ* strain. In summary, the genome-wide screen provides insights into pathways that prevent mislocalization of Cse4 and defines a role for the HIR complex in preventing mislocalization of Cse4 by facilitating proteolysis of Cse4.

Materials and Methods

Yeast strains, plasmids, and SGA analysis

The yeast strains and plasmids used in this study are described in Supplemental Material, Tables S1 and S2. All yeast nonessential gene deletion strains are isogenic to BY4741 unless otherwise indicated. An SGA query strain (YMB6969)

overexpressing *CSE4* in galactose-containing medium was created in Y7092 by homologous recombination using a method described previously (Longtine *et al.* 1998; Baryshnikova *et al.* 2010a). Briefly, PCR products containing HA-tagged *CSE4* driven by the *GAL1* and, separately, MX4-NATR were amplified using DNA from pMB1458 and p4339, respectively. Each PCR product carries a sequence common to the other along with sequences homologous to regions either 5′ or 3′ of the *CSE4* genomic locus. The two purified PCR products were cotransformed into Y7092 (Baryshnikova *et al.* 2010a). Integration of *GALCSE4-HA* into the endogenous locus was verified by PCR, DNA sequencing, Western blot analysis, and the inability of cells to grow on glucose-containing medium. Yeast strain YMB6969 was used to interrogate synthetic fitness defects of Cse4 overexpression with deletions of nonessential genes. SGA screens were performed on galactose-containing medium following the procedures and scoring described previously (Tong *et al.* 2004; Costanzo *et al.* 2010; Z. Li *et al.* 2011). *cac1Δ hir2Δ* and *cac2Δ hir2Δ* strains were derived from meiotic products of diploids of crosses between *cac1Δ*::*KAN* and *hir2Δ*::*NAT* (YMB8785), and *cac2Δ*::*KAN* and *hir2Δ*::*NAT*, respectively, in the BY4741 background. Strain YMB8886 (Δ16 H2A-H2B Δ16 H3-H4) was created by integrating pAB157 and pAB95 sequentially into a wild-type (WT) strain carrying HA-tagged Cse4 expressed from the *GAL1* promoter (YMB6714).

Protein stability assays

Protein stability assays were performed as described previously with minor modifications (Au *et al.* 2008). Briefly, yeast cultures grown in media containing 2% raffinose were supplemented with galactose to a final concentration of 2% to induce the expression of proteins regulated by the *GAL1* promoter at 30° for 2 hr or as described. Subsequently, 2% glucose was added to inhibit transcription and cycloheximide (CHX, 10 μg/ml) to block protein translation. An equal number of cells as measured by OD_{600} were collected at different time points, and whole cell extracts were prepared by the TCA method described previously (Kastenmayer *et al.* 2006). Protein concentrations were determined using a Bio-Rad DC Protein Assay (Cat# 500-0113; Bio-Rad), and equal amounts of protein were separated on a 4–12% Bis-Tris gel (Invitrogen) for western blot analysis. Primary antibodies were anti-HA (clone 12CA5; Roche) and anti-Tub2 (custom made by the Basrai laboratory). Secondary antibodies from Amersham Biosciences were HRP-conjugated sheep α-mouse IgG (NA931V) and HRP-conjugated donkey α-rabbit IgG (NA934V). Western blots were quantified using the SynGene program (SynGene, Cambridge, UK) or ImageJ (Schneider *et al.* 2012) software. Protein half-life was calculated as previously described (Au *et al.* 2013) where least squares regression of percentage remaining (log scale) *vs.* time was used. Values for half-life were derived from three biological replicates unless otherwise noted and were reported as the average ± SE.

Chromosome spreads for localization of Cse4 and Mtw1-GFP

Chromosome spreads were performed as described previously (Collins *et al.* 2004). Strains were grown in SC-Ura containing 2% raffinose until mid-log phase prior to the induction of Cse4 expression by 2% galactose for 1 hr. Anti-HA (1:2500 dilutions) was used as primary antibody (MMS-101P; Covance, Babco) and Cy3 conjugated Goat α-mouse (1:5000 dilutions) as secondary antibody (115165003; Jackson ImmunoResearch Laboratories). Nuclear mass was visualized by 4′,6-diamidino-2-phenylindole (DAPI) staining (1 μg/ml in phosphate-buffered saline (PBS)). For Mtw1-GFP visualization, cells were grown as described above, treated or untreated with 0.5% formaldehyde on ice, stained with DAPI (1 μg/ml in PBS), and examined by fluorescent microscopy. Cells were observed under an Axioskop 2 (Zeiss) fluorescence microscope equipped with a Plan-APOCHROMAT 100X or 63X (Zeiss) oil immersion lens. Image acquisition and processing were performed with the IP Lab version 3.9.9 r3 software (Scanalytics).

ChIP and ChIP-seq experiments

Chromatin immunoprecipitation (ChIP) was performed as described previously (Mishra *et al.* 2007, 2011, 2018) with minor modifications. WT and *hir2Δ* strains carrying *GALCSE4-HA* (pMB1458) were grown logarithmically in 500 ml of 1× SC-URA with galactose and raffinose (2% each) for 6 hr at 30°. Cells were cross-linked in 1% formaldehyde at room temperature for 15 min, quenched in 125 mM glycine for 5 min, and collected by centrifugation. Cells were washed in TBS (20 mM Tris-HCl pH 7.6, 150 mM NaCl), resuspended in spheroplasting buffer (1.2 M sorbitol, 20 mM Na-Hepes, pH 7.4) with Zymolase 100T, and incubated at 30°. Spheroplasts were washed in postspheroplasting buffer (1.2 M sorbitol, 1 mM $MgCl_2$, 20 mM Na-Pipes, pH 6.8), followed by three washes with FA buffer (50 mM Na-Hepes pH 7.6, 1 mM EDTA, 1% Triton X-100, 150 mM NaCl, 0.1% Na-deoxycholate) containing protease inhibitors (P8215; Sigma). Spheroplasts were then suspended in FA buffer with protease inhibitors and sonicated on ice for eight 12-sec bursts applied at an interval of 2 min with an output cycle setting fixed at 30% to obtain an average DNA fragment size of 300–400 bp. One-tenth of the resulting soluble, sheared chromatin fraction was collected as input, and the remaining was incubated with α-HA conjugated agarose beads (A2220; Sigma) at 4° for ∼16 hr. Beads were collected by centrifugation and washed at room temperature with FA buffer for 5 min (three times), FA-HS buffer (50 mM Na-Hepes pH 7.6, 1 mM EDTA, 1% Triton X-100, 500 mM NaCl, 0.1% Na-deoxycholate) for 5 min (twice) and RIPA buffer (10 mM Tris-HCl pH 8.0, 250 mM LiCl, 0.5% NP-40, 1 mM EDTA, 0.5% Na-deoxycholate) for 5 min (twice) followed by 1× TE pH 8.0 for 5 min (twice). Immunoprecipitated DNA was eluted in elution buffer (25 mM Tris-HCl pH 7.6, 10 mM EDTA, 0.5% SDS). Input and immunoprecipitated samples

were recovered after cross-link reversal at 65° for ~16 hr, RNase A and proteinase K treatments, and final purification using Qiagen DNA purification columns (Qiagen). ChIP-qPCR was performed with the 7500 Fast Real Time PCR System using Fast SYBR Green Master Mix (Applied Biosystems) and primers listed in Table S3 with the following conditions: 95° for 20 sec followed by 40 cycles of 95° for 3 sec, 60° for 30 sec. The enrichment values are shown as % input, determined using the $_{dd}C_T$ method (Livak and Schmittgen 2001).

ChIP DNA was used to construct sequencing libraries as described previously (Grøntved *et al.* 2015). Downstream analysis was performed as follows: unfiltered sequencing reads were aligned to the *S. cerevisiae* reference genome (SacCer3) using bwa (Seoighe and Wolfe 1999), allowing up to one mismatch for each aligned read. Reads mapping to multiple sites were retained to allow evaluation of associations with nonunique sequences (Seoighe and Wolfe 1999) and duplicate reads were retained. Binding sites were identified using SICER (Zang *et al.* 2009) with the following parameters: effective genome size 0.97 (97% of the yeast genome is mappable), window size 50 bp, and gap size 50 bp. Calculation of coverage, comparisons between different data sets and identification of overlapping binding regions were preceded by library size normalization and were performed with the "chipseq" and "Genomic Ranges" packages in Bioconductor (Gentleman *et al.* 2004). Control subtraction was carried out in the following way: coverage (exp)/N1−coverage (control)/N2, in which "exp" is the data set (in .bam format) to be examined, N1 is the library size of the experimental data ("exp"), and N2 is the library size of the control. In this study, input sequences (DNA sequences after sonication prior to immunoprecipitation) were used as the control. Occupancy profiles showing reads per million (RPM) normalized to total library size were generated using the Integrative Genomics Viewer (Robinson *et al.* 2011).

Immunoprecipitation experiments

Immunoprecipitation experiments were performed as described previously (Mishra *et al.* 2016, 2018). Briefly, cell pellets collected from yeast strains (40–50 OD_{600} of cells) grown using media and growth conditions described above were dissolved in 500 µl lysis buffer (50 mM Tris pH 7.5, 10% glycerol, 150 mM NaCl, 1 mM DTT, 0.4% NP-40, 1 mM PMSF, and protease inhibitor cocktails Sigma P8215) and bead-beaten (four times) with lysing matrix C glass beads (MP Biomedicals) using the manufacturer's recommended program in a FastPrep-24 5G homogenizer (MP Biomedicals). After centrifugation, protein concentration of the resulting whole cell extracts was measured, and equal amounts of protein from each sample was incubated with rabbit IgG agarose (A2909; Sigma) overnight, followed by washing in TBST (20 mM Tris-HCl, 0.8% NaCl, 0.1% Tween-20) and elution in 2× Laemmli buffer (Invitrogen). Immunoprecipitates were assayed by Western blot analysis using α-TAP (CAB1001; Thermo Scientific) and α-HA (11583816001; Sigma) antibodies.

Subcellular fractionation

Whole cell extract (WCE), soluble and chromatin fractions of WT and *hir2Δ* strains were prepared as described previously (Au *et al.* 2008). Cells grown logarithmically in raffinose-containing medium were induced with 2% galactose for 30 min, followed by addition of cycloheximide at 10 µg/ml for 15 min. Protein samples were normalized based on equal OD_{600} of cells, separated by gel electrophoresis, transferred to nitrocellulose membrane and probed using α-HA antibody. Tub2 and histone H3 (ab1791; Abcam) were used as loading controls for soluble and chromatin fractions, respectively.

Loss of centromere-containing plasmid

Yeast strains containing plasmid pRS416 (*CEN URA3*) were grown at 30° in SC-URA glucose medium for ~16 hr and an equal OD_{600} of cells from each strain were plated on SC-URA glucose (2%) and YPD plates (G_0). To measure the frequency of plasmid loss, 0.05 OD_{600} of cells from each strain were inoculated into 50 ml of YPD and grown nonselectively at 30° for ~10 generations (G_{10}). Equal OD_{600} of cells from G_{10} cultures were then plated as for G_0. The frequency of plasmid segregation was determined as a ratio of total number of colonies on selective SC-URA over nonselective YPD plates, where the values from G_0 for each strain were normalized to 100%. Three biological replicates were performed for each strain and at least 1200 cells at G_0 and G_{10} were plated.

Data availability

Deep sequencing data generated for this study has been deposited in the Gene Expression Omnibus (https://www.ncbi.nlm.nih.gov/geo/) under accession number SRP153412. Supplemental material available at Figshare: https://doi.org/10.25386/genetics.6709553.

Results

A genome-wide SGA screen for gene deletions that show SDL with GALCSE4

Deletions of *PSH1*, *SLX5*, and *RCY1*, which are defective in proteolysis of Cse4, exhibit SDL with overexpressed Cse4 (*GALCSE4*) (Ranjitkar *et al.* 2010; Au *et al.* 2013; Cheng *et al.* 2016; Ohkuni *et al.* 2016). We performed a genetic screen using a SGA to identify gene deletions that display SDL with *GALCSE4*. A query strain with *GALCSE4* integrated in the genome was mated to an array of 4293 individual nonessential gene deletion strains (3620 of which passed quality control filters), and growth of haploid meiotic progeny of each gene deletion with *GALCSE4* was scored on galactose-containing medium. The SGA score for growth was determined as previously described (Baryshnikova *et al.* 2010b) and filtered using the intermediate confidence threshold (P-value <0.05 and |Score| >0.08) (Costanzo *et al.* 2010, 2016). We identified 301 gene deletions that showed a significant growth defect, or SDL, with *GALCSE4*, and refer to them as significant negative genetic interactors (Table S4).

Gene ontology (GO) analysis for biological processes or cellular components for the 301 significant negative genetic interactors was performed using the FunSpec bioinformatics tool (http://funspec.med.utoronto.ca/, April 2017). The analysis was performed using a *P*-value cutoff score of 0.01, and results with a *P*-value $<2.0 \times 10^{-04}$ are displayed. The GO analysis for biological processes showed an enrichment of genes required for DNA replication-independent nucleosome assembly, mitotic sister chromatid cohesion, meiosis, mitosis, and chromosome segregation (Figure 1A). These results are consistent with an enrichment of cellular component GO annotations corresponding to the chromosome, HIR complex, kinetochore, and centromeric region (Figure 1B). Consistent with previous results, *rcy1Δ* (Cheng *et al.* 2016), but not *cac2Δ* were identified as negative genetic interactors with *GALCSE4*. The top 15 negative genetic interactors are listed in Figure 1C, the majority of which are evolutionarily conserved with homologs in human (H), mouse (M), *Drosophila melanogaster* (*D*) and/or *Caenorhabditis elegans* (*C*). The identification of *psh1Δ* as the most significant negative genetic interactor when Cse4 is overexpressed serves as proof of principle for the screen (Ranjitkar *et al.* 2010; Au *et al.* 2013). Among the top 15 negative genetic interactors are all four genes that encode the DNA replication-independent histone chaperone (HIR) complex, namely *HIR1*, *HIR2*, *HIR3*, and *HPC2*.

The genetic interaction profile of GALCSE4 correlates with that of kinetochore mutants

To identify cellular functions impacted by overexpressed Cse4, we performed a genetic correlation analysis looking for similarity between the profile of *GALCSE4* and the complete set of query mutant profiles from the SGA dataset (Costanzo *et al.* 2016). A positive correlation between two mutants' genetic interaction profiles suggests functional similarity between the effects of the genetic perturbations. A list of the top 11 query genes ranked according to their Pearson correlation similarity to the profile of *GALCSE4* is shown in Figure 2A. GO analysis of these 11 genes revealed that there is an enrichment for components of the chromosome, centromere region, and kinetochore (*DSN1*, *AME1*, *NNF1*, *DAM1*, and *OKP1*) (Figure 2B). As expected, the kinetochore mutants that show genetic interaction profiles similar to *GALCSE4* (*dam1-1*, *dsn1-7*, *ame1-4*, and *okp1-5*) also exhibit negative genetic interactions with other kinetochore mutants, namely *iml3*, *mcm21*, *ctf19*, *chl4*, *mcm22*, *ctf3*, and *mcm16* (Figure 2C, red area). Furthermore, *okp1-5*, *ame1-4*, and *dsn1-7* exhibit negative genetic interactions with *hir2Δ*, *hir3Δ*, and *hpc2Δ* strains. Consistent with the role of Cse4 in kinetochore structure and function, these genetic analyses suggest that overexpression of Cse4 contributes to defects in kinetochore function.

HIR complex mutants exhibit SDL with GALCSE4

The HIR proteins function in a complex with Asf1 and Rtt106 for transcriptional repression of histone genes, and the HIR complex serves as the replication-independent chaperone for histones H3 and H4 (Green *et al.* 2005; Fillingham *et al.* 2009; Ferreira *et al.* 2011; Silva *et al.* 2012; Amin *et al.* 2013). In addition to *hir1*Δ, *hir2*Δ, *hir3*Δ, and *hpc2*Δ, we identified *asf1Δ* as a negative genetic interactor with *GALCSE4* (Table S4, SGA score of −0.329 and *P*-value of 1.51e−11). Notably, *rtt106Δ* was not present on the array of yeast deletion strains. To validate the results of the SGA screen, WT, *hir1*Δ, *hir2*Δ, *hir3*Δ, *hpc2*Δ, *asf1Δ*, and *rtt106Δ* strains were transformed with *GALCSE4* or empty vector and examined for growth on glucose or galactose plates. Consistent with the results of the screen, *hir1*Δ, *hir2*Δ, *hir3*Δ, *hpc2*Δ, *asf1Δ*, and *rtt106Δ* strains exhibit SDL with *GALCSE4* on galactose plates (Figure 3A). No growth defects were observed for strains transformed with vector alone on galactose plates. Our previous studies showed that the N-terminus of Cse4 is required for its Ub-mediated proteolysis, so we asked if the N-terminus of Cse4 is required for the SDL of *GALCSE4*. Growth assays showed that *hir1*Δ, *hir2*Δ, *hir3*Δ, *hpc2*Δ, *asf1Δ*, and *rtt106Δ* strains transformed with *GALcse4Δ129* (deletion of the N-terminal 129 amino acids) show slightly reduced growth when compared to vector alone but do not exhibit a SDL phenotype (Figure 3A).

Previous studies have shown that *cac1Δ hir1Δ* strains, but not *cac1Δ* nor *hir1Δ* single mutants, show mislocalization of endogenous Cse4 and chromosome loss (Lopes da Rosa *et al.* 2011). Our results with *hir* mutants prompted us to examine the growth of *cac1Δ*, *cac2Δ*, *cac1Δ hir2Δ*, and *cac2Δ hir2Δ* strains overexpressing *CSE4*. We determined that *cac1Δ hir2Δ* and *cac2Δ hir2Δ* exhibit SDL with *GALCSE4*, but deletion of *CAC1* or *CAC2* does not exhibit SDL with *GALCSE4* (Figure 3B). To investigate the possible role of the HIR complex in proteolysis of Cse4, we focused on Hir2, as the genetic interaction profiles of *HIR2*, *HIR3*, and *HPC2* have higher positive correlations than that of *HIR1* (Usaj *et al.* 2017). We determined that the SDL of *GALCSE4* was linked to *hir2Δ*, as the growth defect of the *hir2Δ GALCSE4* strain on galactose medium was suppressed by expressing *HIR2* on a plasmid (Figure 3C).

Hir2 regulates proteolysis of Cse4

To investigate the cause(s) of the SDL observed when Cse4 is overexpressed in a *hir2Δ* strain, we examined the protein stability of *GALCSE4* in a *hir2Δ* strain after 2.5 hr of induction in galactose medium followed by addition of glucose and the protein synthesis inhibitor cycloheximide (CHX). Western blot analysis of whole cell extracts prepared at different time points after CHX treatment showed that Cse4 was rapidly degraded in the WT strain ($t_{1/2}$ = 16 ± 3 min), but the stability of Cse4 was significantly higher in the *hir2*Δ strain ($t_{1/2}$ = 136 ± 22 min, *P*-value = 0.0055) (Figure 4, A and B). As expected, deletion of another HIR complex component, Hir1, also resulted in stabilization of Cse4 ($t_{1/2}$ = 96 ± 19 min) (Figure S1). Stabilization and mislocalization of overexpressed Cse4 have been observed in *psh1Δ* strains that exhibit SDL with *GALCSE4* (Ranjitkar

A

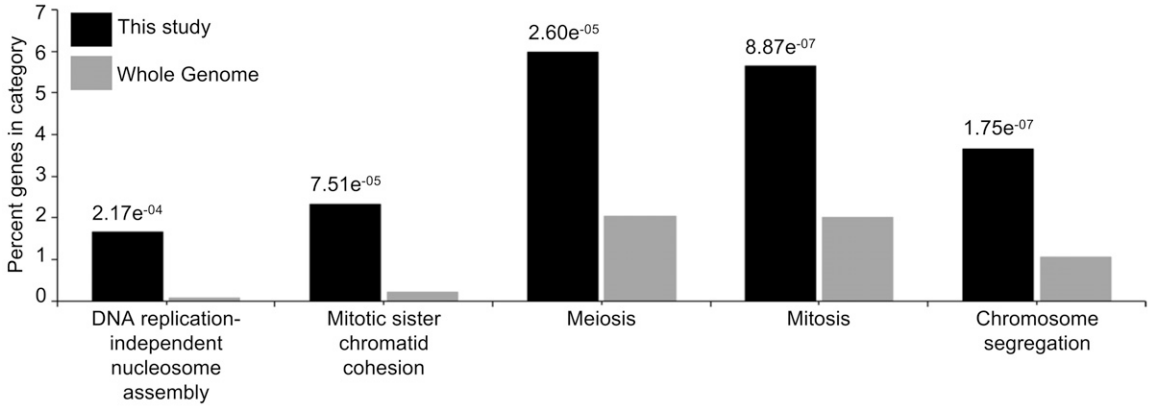

B

Cellular component	Gene	Fraction	p-value
Chromosome	*CHL4 CST9 CTF3 CTF19 HHT1 HIR1 HOP1 HTA1 HTA2 IML3 MCM16 MCM21 MCM22 NKP1 NKP2 SLK19 SMC2 SPO11 SWD1 TEL1*	20/130	1.08e-06
HIR complex	*HIR1 HIR2 HIR3 HPC2*	4/4	3.96e-06
Kinetochore	*BIK1 CHL4 CTF3 CTF19 IML3 MCM16 MCM21 MCM22 NKP1 NKP2 SLK19*	11/48	6.24e-06
Condensed chromosome kinetochore	*CHL4 CTF3 CTF19 IML3 MCM16 MCM21 MCM22 NKP1 NKP2 SLK19*	10/40	7.20e-06
Chromosome, centromeric region	*CHL4 CTF3 CTF19 HIR1 IML3 MCM16 MCM21 MCM22 NKP1 NKP2 PSH1 SLK19*	12/61	1.27e-05

C

Rank	Gene	SGA Score	Homologs*
1	*PSH1*	-0.848	H, M
2	*BLM10*	-0.804	H, M, C
3	*HIR3*	-0.749	H, M
4	*CHS3*	-0.746	C, D
5	*PGM2*	-0.732	C, D, H, M
6	*HIR2*	-0.728	C, D, H, M
7	*YCR090C*	-0.697	C, D, H, M
8	*NKP1*	-0.659	
9	*HPC2*	-0.654	D, H, M
10	*YLR287C*	-0.652	H, M
11	*BUD19*	-0.648	
12	*YRA2*	-0.625	
13	*RNH201*	-0.623	C, D, H, M
14	*HIR1*	-0.621	C, D, H, M
15	*ARO1*	-0.593	

*Homolog information derived from YeastMine database (http://yeastmine.yeastgenome.org/yeastmine/begin.do)

Figure 1 Gene ontology (GO) analysis of negative genetic interactors identified in the SGA screen with *GALCSE4*. (A and B) GO analysis for biological processes (A) or cellular components (B) for the 301 significant negative genetic interactors using the FunSpec bioinformatics tool (http://funspec.med.utoronto.ca/, April 2017). Analysis was performed using a *P*-value cutoff score of 0.01 and results with a *P*-value $<2.0e^{-04}$ are displayed. The *P*-value represents the likelihood of candidate genes from the screen intersecting with the specified category. The percentage denotes the number of genes found in a given category over the number of input genes. The fraction denotes the number of candidate genes over the number of genes annotated within the category. The GO annotation representing genes associated with a particular cellular component or biological process are described. (C) List of the top 15 negative genetic interactors identified in the SGA screen with *GALCSE4*. Listed are the gene name, SGA score and homologs denoted as H, human; M, mouse; D, *Drosophila melanogaster*; C, *Caenorhabditis elegans*. The SGA score is the epsilon value calculated as previously described (Costanzo *et al.* 2010, 2016).

et al. 2010; Au *et al.* 2013). We therefore examined the role of Psh1 in Hir2-mediated Cse4 proteolysis by measuring the stability of Cse4 in a *hir2Δ psh1Δ* strain. Consistent with previous reports (Hewawasam *et al.* 2010; Ranjitkar *et al.* 2010; Au *et al.* 2013), Cse4 levels were relatively stable in *psh1Δ* ($t_{1/2}$ = 63 ± 9 min); however, no significant difference in Cse4 stability was observed between *hir2Δ* ($t_{1/2}$ = 136 ± 22 min) and *hir2Δ psh1Δ* ($t_{1/2}$ = 121 ± 9 min; *P*-value = 0.56) strains (Figure 4B). Taken together, these results indicate that Psh1 contributes to the Cse4 proteolysis defects in *hir2Δ* strains.

Defects in Cse4 proteolysis in hir2Δ strains are not due to constitutive expression of core histones

Transcription of histone genes is tightly regulated in a cell cycle-dependent manner (Osley 1991; Gunjan *et al.* 2005). In addition to its histone chaperone function, the HIR complex acts as a transcriptional corepressor by suppressing the expression of core histones outside of the S phase of the cell cycle (Osley and Lycan 1987; Spector *et al.* 1997; Green *et al.* 2005). To investigate the contribution of mis-regulated histone expression to the defects of Cse4 proteolysis in *hir2Δ*

A

Query allele 1	Query allele 2	Correlation
GALCSE4	*dsn1-7*	0.155
GALCSE4	*ogg1*	0.149
GALCSE4	*isa1*	0.143
GALCSE4	*tfb1*	0.139
GALCSE4	*ame1-4*	0.134
GALCSE4	*cdc20-2*	0.131
GALCSE4	*nnf1-48*	0.131
GALCSE4	*mit1*	0.129
GALCSE4	*yjl118w*	0.129
GALCSE4	*dam1-1*	0.128
GALCSE4	*okp1-5*	0.128

Red: kinetochore mutants

B GO analysis for component

GO terminology	Cluster frequency	*p*-value
Chromosome, centromeric region	6 out of 11 genes, 54.5%	$5.21e^{-08}$
Condensed nuclear chromosome, kinetochore	5 out of 11 genes, 45.5%	$3.95e^{-07}$

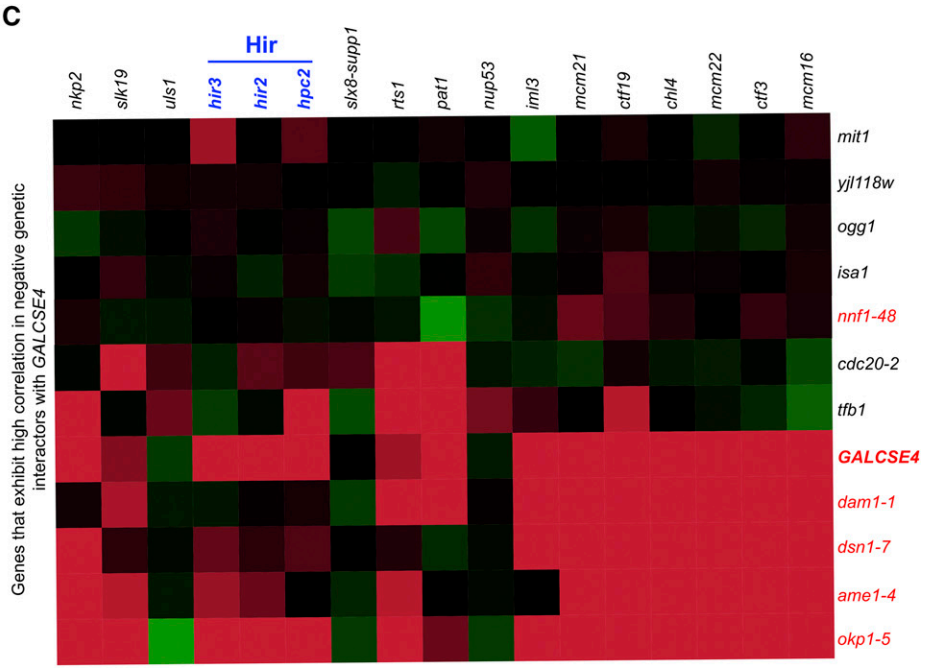

Figure 2 The genetic interaction profile of *GALCSE4* is similar to that of kinetochore mutants. (A) *GALCSE4* exhibits a genetic interaction profile similar to profiles displayed by kinetochore mutants. Shown is a list of 11 mutants showing the most similar genetic interaction profiles (highest Pearson correlation score) to that of *GALCSE4*. (B) GO analysis for cellular component of genes in (A). (C) Representative heat map showing genetic interactions of the 11 genes listed in (A). Negative and positive genetic interactions are shown in red and green, respectively. The intensity of the color reflects the strength of the genetic interaction. Kinetochore mutants that exhibit high positive correlation with *GALCSE4* from (A) above also exhibit genetic interactions with deletions of genes encoding for the HIR complex, namely *hir2Δ*, *hir3Δ*, and *hpc2Δ*.

cells, we created a strain expressing histones H2A-H2B and H3-H4 (*Δ16 H2A H2B*, *Δ16 H3 H4*) from a mutant *hta1-htb1* promoter lacking a 16-bp negative regulatory element (*Δ16*) functionally targeted by HIR (Osley *et al.* 1986; Lycan *et al.* 1987; Bortvin and Winston 1996), thus mimicking the transcription of core histones outside of S phase as observed in *hir2Δ* cells. As expected, the WT strain showed reduced levels of H2B and H3 upon HU treatment (Xu *et al.* 1992; DeSilva *et al.* 1998). In contrast, the levels of H3 and H2B were not repressed in HU treated *Δ16 H2A H2B*, *Δ16 H3 H4* cells (Xu *et al.* 1992; DeSilva *et al.* 1998) (Figure 4C). Protein stability assays showed that proteolysis of transiently overexpressed Cse4 in the *Δ16 H2A H2B*, *Δ16 H3 H4* strain ($t_{1/2}$ = 49 ± 3 min) was similar to the WT strain ($t_{1/2}$ = 46 ± 12 min) (Figure 4D). We conclude that constitutive expression of histones in the *hir2Δ* strain does not contribute to defects in Cse4 proteolysis.

Hir2 prevents mislocalization of Cse4 to noncentromeric regions

Previous studies have shown that increased stability of Cse4 in *psh1Δ* and *slx5Δ* strains correlate with its mislocalization to noncentromeric regions (Hewawasam *et al.* 2010; Ranjitkar *et al.* 2010; Au *et al.* 2013; Hildebrand and Biggins 2016; Ohkuni *et al.* 2016). We performed chromosome spreads, a technique that removes soluble material, to examine the localization of chromatin-bound Cse4 in *hir2Δ* strains. Immunofluorescence staining of HA-Cse4 showed one to two discrete Cse4 foci (red) coincident with DAPI signal (blue) in a wild type strain (Figure 5A). In contrast, HA-Cse4 signals were largely diffused across the nuclear mass in the *hir2Δ* strain (Figure 5A). The percentage of *hir2Δ* cells showing mislocalization of Cse4 signals was about fourfold higher (~87%) compared to that observed in the WT strain (~22%) (Figure 5B). We also examined if the localization of another kinetochore protein, Mtw1 (tagged with GFP), was affected in the *hir2Δ* strain. In contrast to Cse4, Mtw1-GFP localized to one to two discrete foci within the DAPI-stained DNA in 97 and 98% of WT and *hir2Δ* strains, respectively (Figure S2). We next performed subcellular fractionation and assayed the stability of Cse4 in WCE, soluble, and chromatin fractions after treatment with CHX (Figure 5, C and D). Cse4 levels were significantly decreased in all fractions in a WT strain after treatment with CHX. In contrast, steady-state levels (T_0) of Cse4 were high in all fractions in the *hir2Δ* strain, but the levels in WCE and chromatin fractions remained high in the *hir2Δ* strain after treatment with CHX. Taken together, these results show that overexpressed Cse4 is preferentially enriched and more stable in chromatin and is mislocalized to noncentromeric regions in the *hir2Δ* strain.

Mislocalized Cse4 is enriched at promoter regions in hir2Δ strains

Genome-wide ChIP-seq experiments were performed to identify the chromosomal sites of Cse4 mislocalization in *hir2Δ*

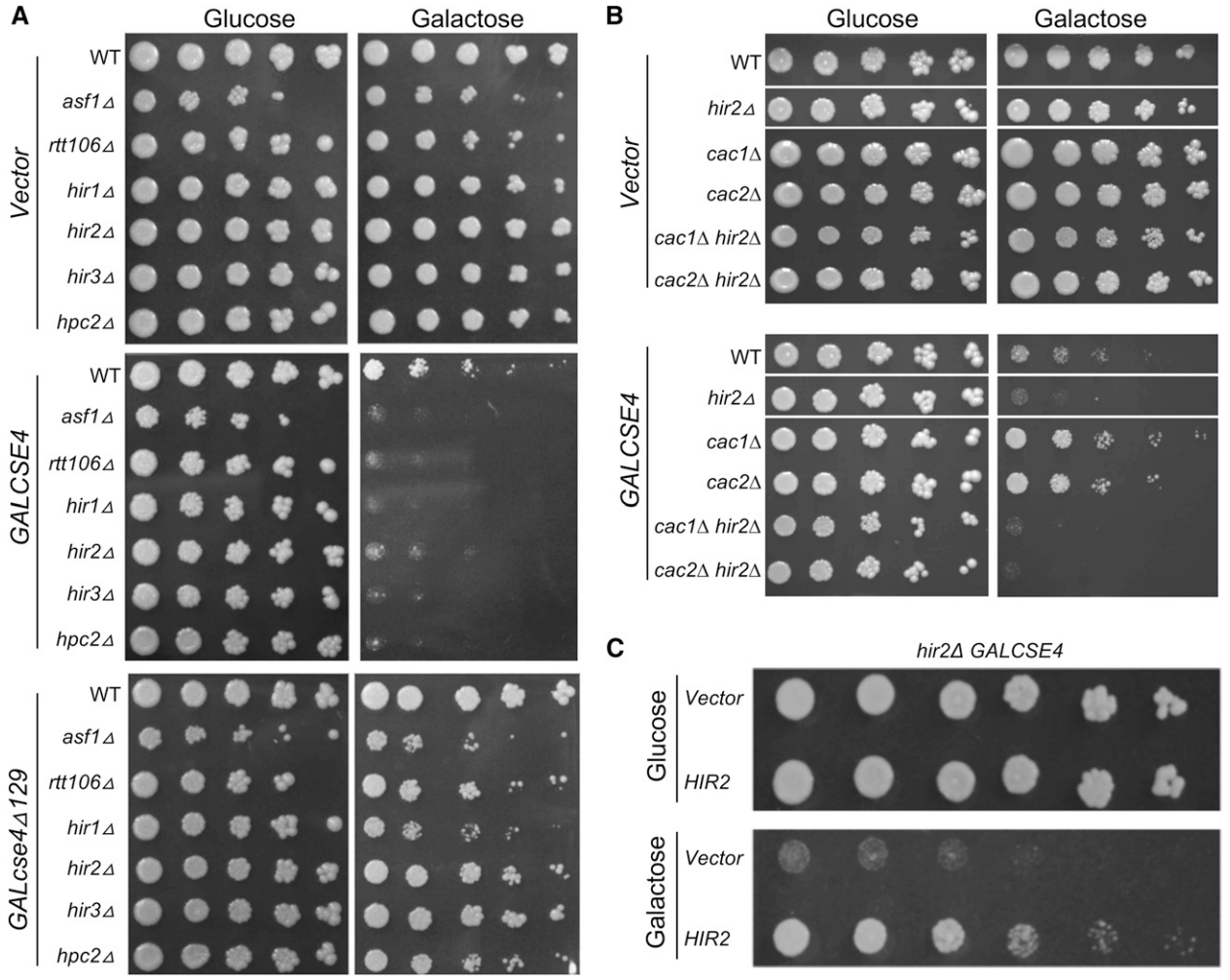

Figure 3 HIR complex mutants exhibit SDL with *GALCSE4*. (A) Overexpression of Cse4 causes lethality in mutants of the HIR complex mediated by the N-terminus of Cse4. Wild type (WT) (BY4741) and the isogenic deletion strains as indicated were transformed with vector (pMB433), *GALCSE4HA* (pMB1458), and *cse4Δ129* (*GALcse4Δ129HA*; pMB1459). Serial dilutions (fivefold) of each strain with the indicated plasmid were plated on SC-Ura plates containing either glucose (2%) or galactose and raffinose (2% each). Plates were photographed after 2–5 days of growth at 30°. At least three independent transformants were examined for each strain. (B) Deletion of *CAC1* or *CAC2* does not suppress the lethality of *hir2Δ* overexpressing Cse4. *cac1Δ hir2Δ* (YMB10463) and *cac2Δ hir2Δ* (YMB10464) strains were transformed with pMB1458 or empty vector. The growth of the these transformants were determined on galactose-containing medium in fivefold serial dilution and grown as indicated in (A). Corresponding WT, *hir2Δ*, *cac1Δ*, and *cac2Δ* strains were used as controls. (C) Complementation of *GALCSE4* induces lethality in a *hir2Δ* strain by plasmid-borne *HIR2*. A *hir2Δ* strain carrying *GALCSE4HA* (pMB1458) was transformed with a plasmid containing either *HIR2* (MoBy 2μ library; GE Dharmacon) or vector control. Serial dilutions (fivefold) of each strain with the indicated plasmid were plated on selective plates containing either glucose (2%) or galactose and raffinose (2% each). Plates were photographed after 2–5 days of growth at 30°.

strains. Genomic regions were enriched from formaldehyde-crosslinked, sheared chromatin by immunoprecipitation of HA-Cse4. Sequencing of input and ChIP samples resulted in ~2 million reads/sample, with an average fragment length of ~300 bp. The Cse4-associated genomic regions (peaks) had a median width of 500–800 bp. Representative results for Cse4 peaks at the *CEN* and peri-*CEN* (20 kb flanking *CEN*) from two different chromosomes (1 and 13) are shown in Figure 6. As expected, enrichment of Cse4 was detected at centromeres in WT and *hir2Δ* strains. Cse4 was found mislocalized at some noncentromeric regions in WT cells; however, substantially more noncentromeric peaks were observed in the *hir2Δ* strain (Figure 6, A and B). Enrichment of Cse4 was found at 197 and 1470 genomic regions in WT and *hir2Δ* strains, respectively, with an overlap of ~160 peaks between the two strains (Table S5). Of the 1470 peaks identified in the *hir2Δ* strain, 1047 were at promoter regions (~71%), 153 within gene bodies or terminal regions, and 270 in noncoding intergenic regions; no enrichment of Cse4 was detected at telomeres or transposable elements. The enrichment of Cse4 at promoters was substantially higher in the *hir2Δ* strain compared to that in the WT strain (Figure 6C). Of the 1470 Cse4 peaks in the *hir2Δ* strain, 1411 peaks (96%) overlapped with the Cse4 peaks identified previously in a *psh1Δ* strain overexpressing Cse4 (Figure 6D) (Hildebrand and Biggins 2016).

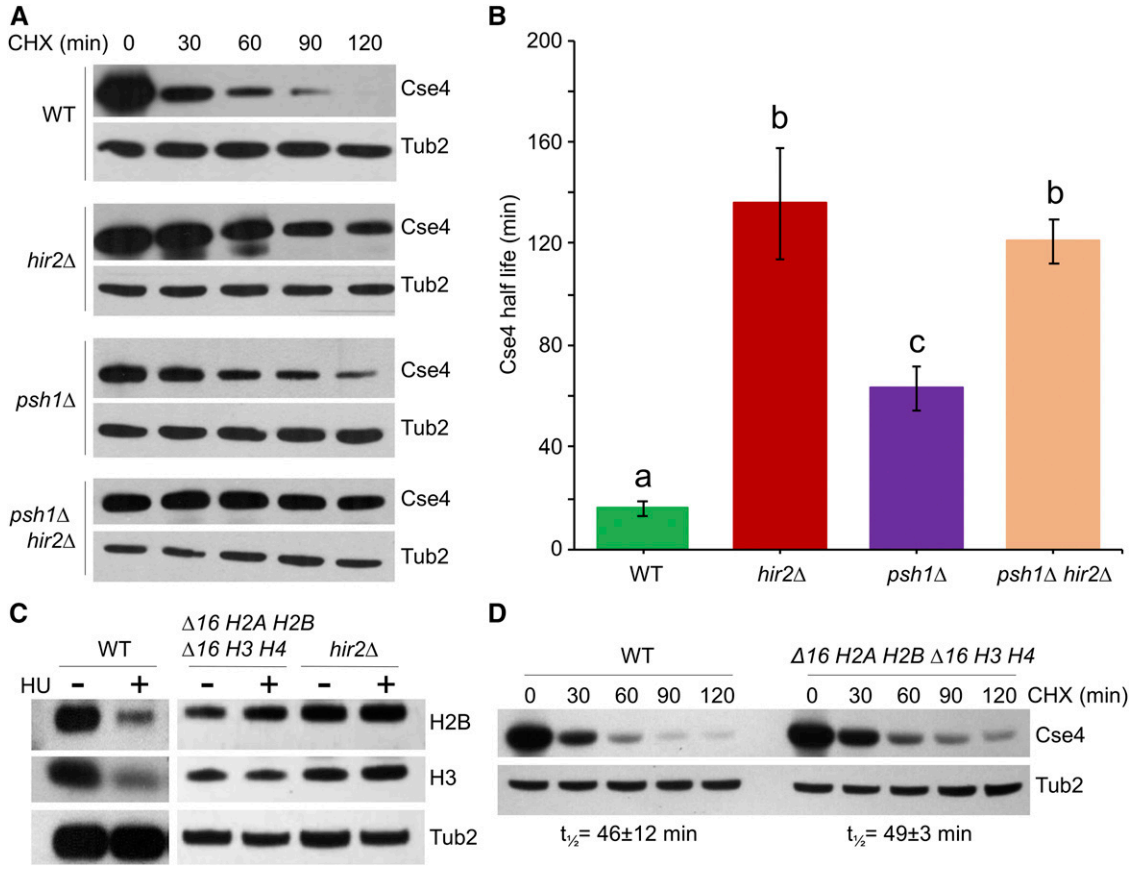

Figure 4 *hir2Δ* strains exhibit defects in proteolysis of Cse4 independent of their effect on core histone gene expression. (A and B) Hir2 regulates proteolysis of Cse4. (A) WT, *hir2Δ*, *psh1Δ*, and *hir2Δ psh1Δ* strains transformed with *GALCSE4HA* (pMB1458) were grown for 2.5 hr at 30° in SC-Ura galactose and raffinose (2% each). Whole cell protein extracts prepared from samples for Western blot analysis were collected at indicated time points before and after the addition of cycloheximide (CHX, 10 μg/ml) and glucose (2%). Blots were probed with α-HA antibodies for Cse4 detection and α-Tub2 (loading control). (B) Half-life ($t_{1/2}$) of Cse4 was calculated from Western blots described in (A). The average from three independent experiments ± SE is shown. Values sharing the same letter (a, b, c) are not significantly different at the 5% level based on ANOVA (*P*-values: WT *vs. hir2Δ*, 0.0055; WT *vs. psh1Δ*, 0.0067; *hir2Δ vs. psh1Δ*, 0.0362; *hir2Δ vs. hir2Δ psh1Δ*, 0.558; *psh1Δ vs. hir2Δ psh1Δ*, 0.0093). (C) Deletion of regulatory elements within histone promoters lead to constitutive expression of core histones similar to *hir2Δ* strains. WT (YMB6714), *hir2Δ* (YMB7693), and *Δ16 H2A H2B Δ16 H3 H4* (YMB8886) strains were transformed with *GALCSE4HA* (pMB1458) and grown in YPD medium with and without hydroxyurea (HU, 0.1 M) for 90 min. Protein blots of whole cell extracts were probed with α-H2B (ab1790; Abcam), α-H3 (ab1791; Abcam), and α-Tub2 (loading control). (D) Constitutive expression of core histones does not contribute to defects in Cse4 proteolysis. Western blot analysis of protein extracts prepared from WT (YMB6714) and Δ16 H2A H2B Δ16 H3 H4 (YMB8886) strains with *GALCSE4HA* (pMB1458) after growth in galactose-containing medium for 2 hr and shifted to glucose medium (2%) and treated with CHX (10 μg/ml) for the indicated time points. Blots were probed with α-HA and α-Tub2 (loading control) antibodies. Half-life with average deviation from the mean was calculated based on two independent experiments.

We selected a subset of the genomic regions of Cse4 enrichment and performed ChIP-qPCR with WT and *hir2Δ* strains. These included genomic regions representing the *CEN* (*CEN1* and *CEN3*), the peri-*CEN* (R3 and R4), a coding region (R9), ARS (R8), noncoding intergenic regions (R5, R7, and R11), promoters (R6, R10, R12, R13, and R14), and negative controls (R15 and R16). No significant enrichment of Cse4 was detected in WT and *hir2Δ* strains at negative control (R15 and R16) DNA regions, as expected (Figure S3). In agreement with ChIP-seq results, we confirmed significant enrichment of Cse4 at nine out of the 10 noncentromeric regions in *hir2Δ* strains (Figure S3). The higher levels of Cse4 at *CEN* (*CEN1* and *CEN3*) and peri-*CEN* (R4) regions and at the R10 promoter in *hir2Δ* strains were not statistically different from the WT strain (Figure S3). These results validated the ChIP-seq findings and show that Cse4 is mislocalized to noncentromeric regions in *hir2*Δ strains, with a preference for gene promoter regions.

Deletion of *CAC2* has been shown to reduce the deposition of overexpressed Cse4 at promoters of medium to highly expressed genes and to suppress the SDL of a *psh1Δ GALCSE4* strain (Hewawasam *et al.* 2018). Our results showed that deletion of *CAC2* does not suppress the SDL of *hir2Δ GALCSE4* (Figure 3B); therefore, we hypothesized that deletion of *CAC2* would not affect enrichment of Cse4 at promoter regions in the *hir2Δ* strain. Consistent with this, ChIP-qPCR showed that levels of Cse4 at promoter regions in a *hir2Δ* strain were not significantly different than that in *hir2Δ cac2Δ* strains (Figure S4).

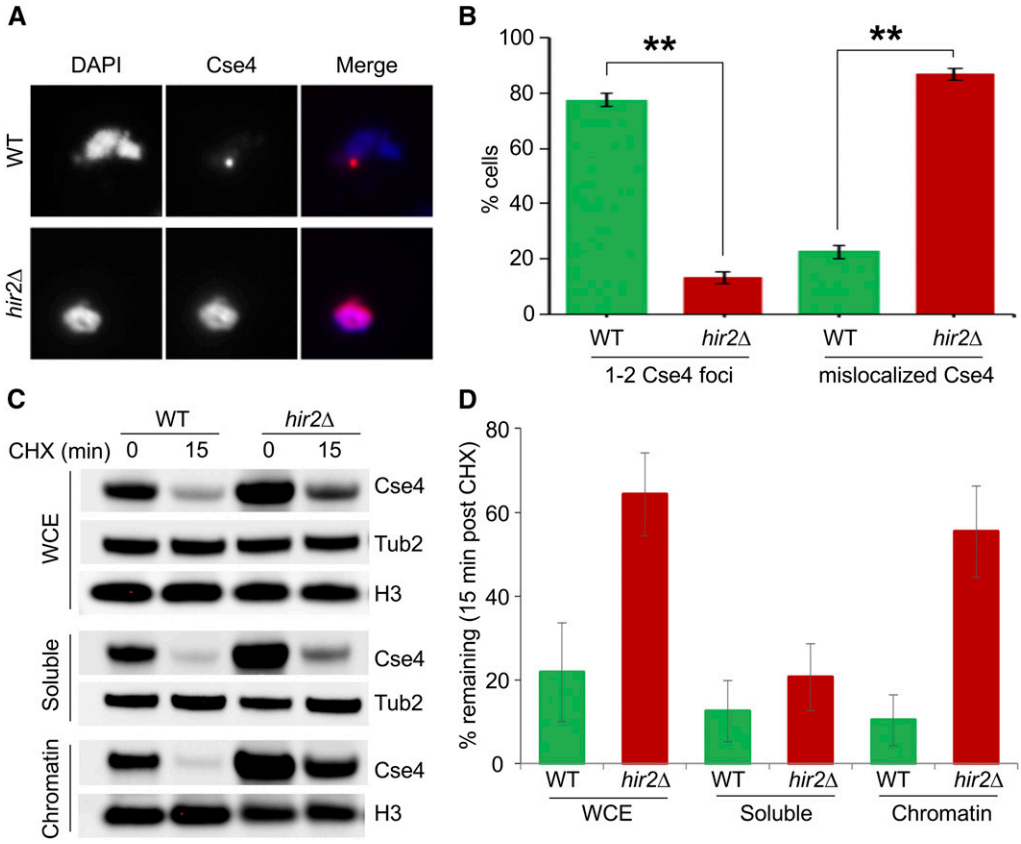

Figure 5 Cse4 mislocalized to noncentromeric regions in *hir2Δ* strains. (A) Cse4 is mislocalized in *hir2Δ* strains. Chromosome spreads were prepared from WT and *hir2Δ* strains with *GALCSE4HA* (pMB1458) grown in SC-Ura containing 2% raffinose. Expression of Cse4 was induced for 1 hr by adding 2% galactose. Chromosome spreads were probed with α-HA (16B12; Covance) primary antibodies followed by Cy3 conjugated Goat α-mouse secondary antibodies for Cse4 detection. Nuclear mass was visualized by DAPI staining. (B) Quantification of Cse4 mislocalization in *hir2Δ* strains. Percentage of cells from chromosome spreads in (A) that exhibit either 1–2 Cse4-foci or dispersed Cse4 signals in WT or *hir2Δ* strains. (C and D) Cse4 is stable in the chromatin fraction from *hir2Δ* strains. The levels and stability of Cse4 in whole cell extract (WCE), soluble, and chromatin fractions were determined by Western blot analysis using α-HA antibody. Expression of Cse4 was induced in WT or *hir2Δ* strains by growth in galactose-containing medium for 30 min followed by treatment with CHX (10 μg/ml) for 15 min. Tub2 and histone H3 were loading controls. (D) Quantification of Cse4 levels from (C). The percentage of Cse4 remaining after CHX treatment (15 min) is calculated taking the t_0 value as 100%. The error bar represents the average deviation from the mean of two independent biological repeats.

Hir2 interacts with Cse4 and facilitates the interaction of Cse4 with Psh1 to promote Cse4 proteolysis

The overlapping mislocalization pattern of Cse4 in *hir2Δ* and *psh1Δ* strains and the similar degree of Cse4 protein stability between the *hir2Δ psh1Δ* and the *hir2Δ* strain prompted us to examine if Hir2 interacts with Cse4 and facilitates the interaction between Cse4 and Psh1. First, coimmunoprecipitation (IP) assays detected a significant interaction (*P*-value = 0.00036) between HA-Cse4 and Hir2-TAP as compared to the nontagged control (Figure 7, A and B). Next, we examined the interaction of Psh1 and Cse4 in WT and *hir2Δ* strains and determined that the interaction between Psh1-TAP and HA-Cse4 was reduced by at least threefold in the *hir2Δ* strains compared to the WT strain (Figure 7, C and D). These results prompted us to examine if overexpression of *PSH1* suppresses the SDL of *GALCSE4* and defects in Cse4 proteolysis in *hir2Δ* strains. Overexpression of *PSH1* suppressed the lethality of *GALCSE4* on galactose medium (Figure 7E, *P*-value = 0.00054) and increased the rate of proteolysis of Cse4 in *hir2Δ* strains by approximately threefold (Figure 7F). We conclude that Hir2 facilitates the interaction between Cse4 and Psh1 and promotes proteolysis of Cse4.

Given the negative genetic interactions of the kinetochore mutant *okp1-5* with *hir3Δ*, *hir2Δ*, and *hpc2Δ* (Figure 2C), and our results showing mislocalization of Cse4 in *hir2Δ* strains, we examined a possible role of the HIR complex in chromosome segregation. The ability of cells to retain a centromere-containing plasmid (pRS416 *URA3*) after nonselective growth for 10 generations was assayed. Our results showed that plasmid retention for *hir2Δ* and *psh1Δ* is 65 and 72%, respectively, compared to 99% for the WT strain. We did not observe a significant difference in plasmid retention for *hir2Δ* (65%) when compared to the *psh1Δ hir2Δ* (58%) strain (Figure 7G). Previous studies have also reported plasmid retention defects in a *psh1Δ* strain (Herrero and Thorpe 2016; Metzger *et al.* 2017). Taken together, our results show that Hir2 facilitates the interaction of Cse4 with Psh1, and this may contribute to the increased plasmid loss in *hir2Δ* strains.

Discussion

To gain a comprehensive understanding of pathways that prevent mislocalization of Cse4, we performed the first genome-wide screen to identify gene deletions that display SDL with *GALCSE4*. The screen identified components of the replication-independent histone chaperone complex HIR (*HIR1*, *HIR2*, *HIR3*, *HPC2*) and a Cse4-specific E3 ubiquitin ligase, *PSH1*, as displaying the highest level of growth sensitivity to *GALCSE4*. Identifying multiple components of the HIR complex emphasizes the biological importance of the HIR

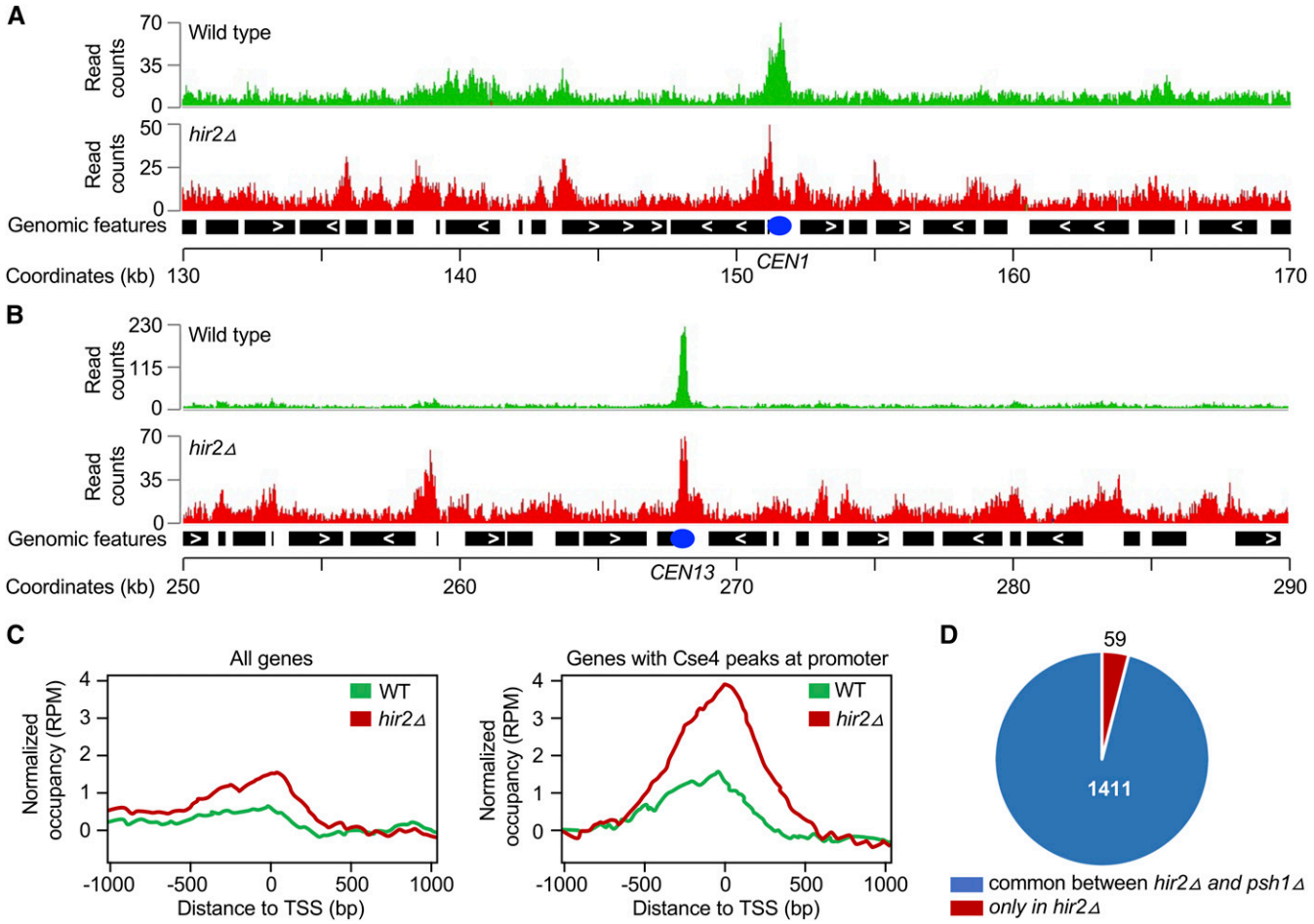

Figure 6 Cse4 is mislocalized to noncentromeric regions in *hir2Δ* strains. ChIP was performed using chromatin prepared from WT and *hir2Δ* strains carrying *GALCSE4HA* (pMB1458) after growth for 6 hr in SC-Ura with galactose and raffinose (2% each). Immunoprecipitation was with α-HA agarose as described in *Materials and Methods*. Input and immunoprecipitated samples were used for ChIP-sequencing as described (Grøntved *et al.* 2015). (A and B) Cse4 is mislocalized to noncentromeric regions in a *hir2Δ* strain. A representative region of the Cse4 ChIP-seq enrichment from WT and *hir2Δ* strains is shown from the chromosome 1 region flanking *CEN* (between 130,000 and 170,000 bp). Peaks of Cse4 after normalization and input subtraction are shown. (B) A representative region of the Cse4 ChIP-seq enrichment from WT and *hir2Δ* strains is shown from the chromosome 13 region flanking *CEN* (between 250,000 and 290,000 bp). Peaks of Cse4 after normalization input subtraction are shown. (C) Mislocalization of overexpressed Cse4 is higher in promoter regions. Average Cse4 ChIP-seq coverage from WT and *hir2Δ* strains calculated from 1000 bp upstream and downstream of transcription start sites (TSS) for all genes or for regions where Cse4 was found to be enriched at promoters. (D) Comparative analysis of genomic regions for Cse4 mislocalization between *hir2Δ* and *psh1Δ* strains. Pie chart denotes the genomic regions associated with mislocalized Cse4 common between *hir2Δ* strain from our study and *psh1Δ* strain identified previously (Hildebrand and Biggins 2016).

complex when Cse4 is overexpressed. We investigated Hir2 to establish the role of the HIR complex in proteolysis and localization of Cse4. Hir2 interacts with Cse4 *in vivo*, and a *hir2Δ* strain shows defects in Cse4 proteolysis, mislocalization of Cse4 to noncentromeric regions, and increased loss of centromere-containing plasmids. In addition to providing insight into evolutionarily conserved pathways that regulate proteolysis of Cse4, the genome-wide screen allowed us to define a novel role for the HIR complex in preventing mislocalization of Cse4 by facilitating proteolysis of Cse4, thereby promoting genome stability.

GO analysis of the negative genetic interactors with *GALCSE4* reveals an enrichment of proteins required for DNA replication-independent nucleosome assembly, sister chromatid cohesion, meiosis and mitosis, and the centromere/kinetochore. Remarkably, 175 of the 301 genes identified (58%) have human homologs, suggesting that pathways regulating cellular levels of Cse4 are evolutionarily conserved. The enrichment of kinetochore proteins and a strong positive correlation of the genetic interaction profile of *GALCSE4* with kinetochore mutants suggests that kinetochore function is impaired when Cse4 is overexpressed. This conclusion is supported by previous results showing higher chromosome loss in *GALCSE4* strains (Au *et al.* 2008; Mishra *et al.* 2011). We observed that *GALCSE4* but not *GALcse4Δ129* results in SDL in the *hir* mutants. The N-terminus of Cse4 has been shown to be essential for its interactions with a subset of kinetochore proteins (Ortiz *et al.* 1999; Chen *et al.* 2000; Morey *et al.* 2004; Au *et al.* 2013; Hornung *et al.* 2014). We propose that the SDL phenotype of *GALCSE4* in *hir* mutants is partly due to titration

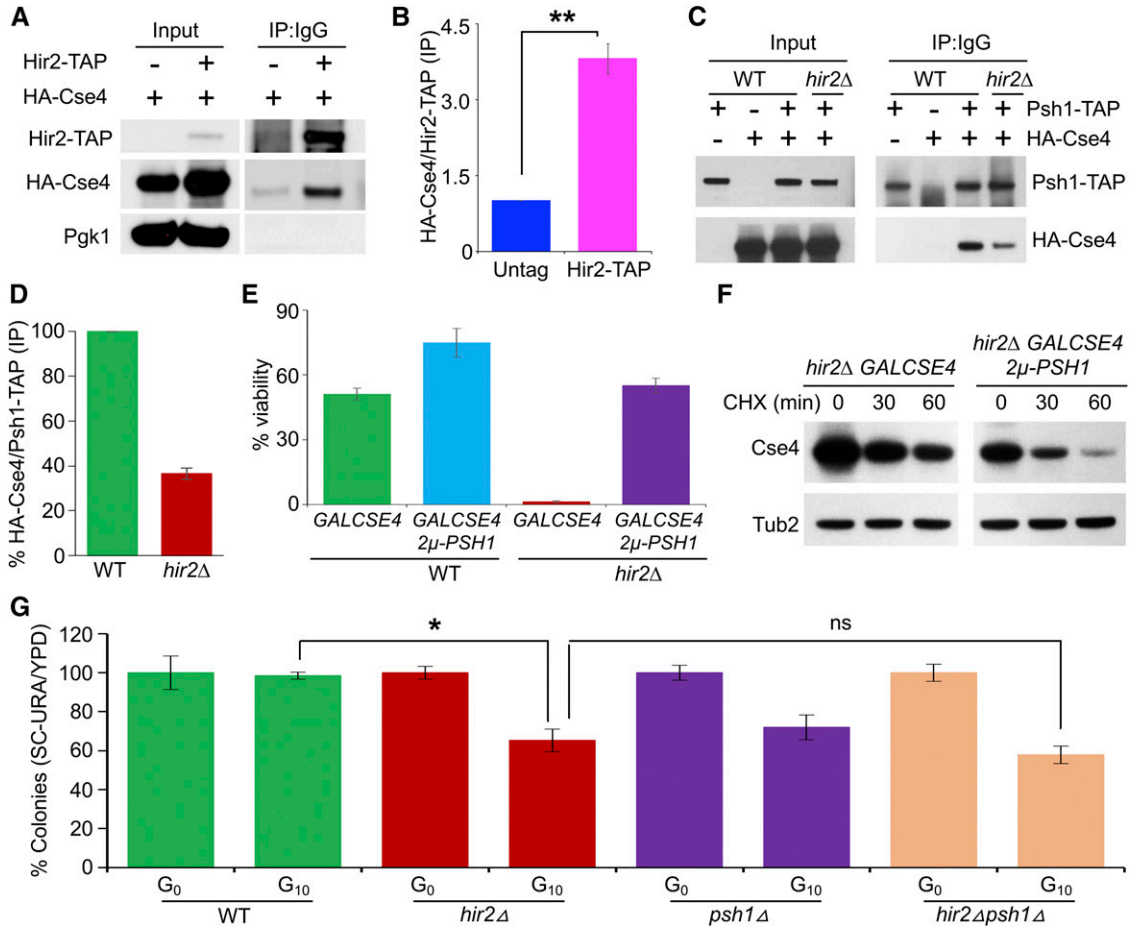

Figure 7 Hir2 interacts with Cse4 and facilitates Psh1-mediated proteolysis of Cse4. (A) Hir2 interacts with Cse4 *in vivo*. Immuno-precipitation (IP) experiments were performed using a *HIR2-TAP* strain (OpenBiosystem) transformed with either *GALCSE4HA* (pMB1597) or vector control. Equal amounts of WCE prepared from strains grown in galactose medium for 2 hr were immunoprecipitated with rabbit IgG agarose to pull down Hir2-TAP. The presence of Cse4HA in the IP was detected by Western blot analysis using α-HA antibody. (B) Quantification of interaction of Cse4 and Hir2 in WT strain. Western blots from (A) were used for quantification, where interaction between Hir2-TAP and Cse4HA was quantitated as fold increase in Cse4HA ratio (IP/Input) of Hir2-TAP strain *vs.* non-TAP strain. Error bar represents SD from three independent experiments. *P*-value was calculated by Student's *t*-test. (C) Reduced interaction of Cse4 and Psh1 in a *hir2Δ* strain. WT, Psh1-TAP (Open Biosystems) or isogenic *hir2Δ* strains transformed with either empty vector (pMB433) or *GALCSE4HA* (pMB1458) were grown logarithmically and Cse4 expression induced by growth in galactose-containing medium for 2 hr. IP experiments were performed as described in (A), and blots were probed with α-HA and α-TAP (CAB1001; Thermo Scientific) antibodies. (D) Quantitation of reduced interaction of Cse4 and Psh1 in *hir2Δ* strain. Western blots from (B) were quantified to determine the interaction between Psh1-TAP and Cse4HA. The ratios showing levels of Cse4HA over Psh1-TAP from co-IP samples were calculated and normalized to a value of 100 for the WT strain. Error bars represent SD from three independent experiments. (E) Overexpression of Psh1 suppresses the lethality caused by *GALCSE4* in *hir2Δ* strains. Viability assays were performed with a *hir2Δ* strain containing *GALCSE4HA* (pMB1458) and *PSH1* (From MoBY 2μ ORF library) or *GALCSE4HA* (pMB1458) and vector alone. A WT strain containing *GALCSE4HA* (pMB1458) was used as a control. About 1200 cells from each strain were plated on glucose- and galactose-containing medium. Viability is calculated as the ratio of colonies on galactose plates over glucose plates. Average ± SD from three independent experiments is shown. ns, not significant (*P*-value = 0.07); ** *P*-value <0.001, Students' *t*-test. (F) Over-expression of Psh1 facilitates proteolysis of Cse4 in *hir2Δ* strains. Western blot analysis was performed using whole cell extracts from *hir2Δ* strains with *GALCSE4HA* (pMB1458) and *2μ-PSH1* or vector control. Expression of Cse4 was induced in galactose (2%)-containing medium for 2 hr at 30° and cells shifted to glucose medium and treated with CHX (10 μg/ml). Stability of Cse4 at various time points post-CHX treatment was determined by Western blot analysis probing with α-HA and α-Tub2 (loading control) antibodies. Two biological repeats were performed, with experimental variation within 10% from the mean. (G) Defects in chromosome segregation in *hir2Δ* strain. Loss of *CEN* containing plasmid (pRS416 *CEN URA3*) was measured in WT, *psh1Δ*, *hir2Δ*, and *psh1Δ hir2Δ* strains. Strains were grown in SC-URA media selecting for the plasmid pRS416 (denoted as generation G_0) followed by dilution and growth in nonselective YPD medium for 10 generations (denoted G_{10}). The frequency of plasmid retention was calculated as the ratio of number of colonies on SC-URA over YPD, where G_0 values for each strain were normalized to 100%. At least 1200 cells for each strain at G_0 and G_{10} were plated and average frequency of plasmid loss ± SD is shown for three biological replicates. ns, not significant (*P*-value = 0.18); * *P*-value = 0.02; Students' *t*-test.

of kinetochore proteins to ectopic sites by interactions with the N-terminal tail of mislocalized full length Cse4. The lack of an obvious SDL of *GALcse4Δ129* in *hir* mutants suggests that even though overexpressed cse4Δ129 is stable (Chen *et al.* 2000; Morey *et al.* 2004; Au *et al.* 2013; Hornung *et al.* 2014) and may be mislocalized, it cannot titrate the kinetochore proteins to ectopic sites to the same extent as full length Cse4. Hence, the N-terminus of Cse4 contributes to the SDL of *GALCSE4*, and

increased stability alone is insufficient for an SDL phenotype. Our studies with human cells have likewise shown that mislocalization of overexpressed CENP-A results in chromosomal instability due to titration of a subset of kinetochore proteins to ectopic noncentromeric regions (Shrestha *et al.* 2017).

Mislocalization of Cse4 and its homologs leads to increased chromosome loss in yeast, flies, and human cells (Heun *et al.* 2006; Au *et al.* 2008; Mishra *et al.* 2011; Shrestha *et al.* 2017), and the extent of Cse4 or CENP-A mislocalization correlates with the level of chromosome loss in yeast and human cells, respectively (Au *et al.* 2008; Shrestha *et al.* 2017). Given the increased stability and mislocalization of Cse4 in *hir2Δ* strains, we investigated the importance of the HIR complex in genome stability. Several observations support a role for the HIR complex in chromosome segregation under normal physiological conditions, *i.e.*, when Cse4 is expressed from its own promoter: (a) an increase in the loss of a centromere-containing plasmid in *hir2Δ* strains; (b) the negative genetic interaction of kinetochore mutants *okp1-5* and *ame1-4* with *hir3Δ*, *hir2Δ* and *hpc2Δ*; (c) the synthetic lethality between *hir2Δ* and *spt4Δ* (Basrai Laboratory, unpublished data), the latter strain exhibiting chromosome segregation defects and mislocalization of Cse4 expressed from its own promoter (Crotti and Basrai 2004); and (d) increased chromosome loss in *hir1Δ cac1Δ* strains showing mislocalization of Cse4 (Lopes da Rosa *et al.* 2011).

Our results show that defects in Cse4 proteolysis observed in WCE of *hir2Δ* strains correlates with the enrichment of Cse4 in the chromatin fraction. Stability of Cse4 in the soluble fractions are not significantly different between WT and *hir2Δ* strains. Consistent with these results, genome-wide ChIP experiments showed mislocalization of Cse4 to noncentromeric regions, with a preferential enrichment at promoter regions in the *hir2Δ* strain. Given the role of the HIR complex in the regulation of replication-dependent expression of histones (Osley 1991; Green *et al.* 2005; Gunjan *et al.* 2005), we asked if the increased stabilization of Cse4 in *hir2Δ* strains was due to misregulation of core histone gene expression. Protein stability assays showed that aberrant regulation of core histone proteins does not contribute to the increased stability of Cse4.

Previously, Lopes da Rosa *et al.* (2011) studied Cse4 mislocalization and stability in *hir1Δ*, *cac1Δ*, and *hir1Δ cac1Δ* double mutants. They found Cse4 half-life to be marginally increased in all three strains compared to WT, but Cse4 mislocalized only in the *hir1Δ cac1Δ* double mutant. They also measured H3 turnover in chromatin and found that both *hir1Δ cac1Δ* and *hir1Δ* mutants exhibited slower turnover rates. Since the sites of extracentromeric Cse4 accumulation in the *hir1Δ cac1Δ* double mutant correlated with sites of rapidly exchanging nucleosomes in WT cells, they concluded that Cse4 mislocalization was primarily due to decreased eviction of Cse4 at extrachromosomal sites, mediated by both HIR and CAF-1, and not Cse4 stability *per se*. That these authors failed to detect Cse4 mislocalization in the *hir1Δ* single mutant could be explained by the fact that they assayed a tagged Cse4 allele expressed at endogenous levels, while in our experiments Cse4 was overexpressed. Notably, a recent study under conditions of Cse4 overexpression showed that *cac1Δ* reduces Cse4 chromatin deposition genome-wide and suppresses the SDL of *psh1Δ* (Hewawasam *et al.* 2018), effects opposite to that observed under the experimental conditions of Lopes da Rosa *et al.* (2011). We do not rule out a role for the HIR complex in mediating removal of Cse4 at extrachromosomal sites; however, our results indicate additional functions of HIR in regulating proteolysis of Cse4 independently of the CAF-1 complex.

Stringent regulation of histone H3 (Singh *et al.* 2012) and p53 (Love and Grossman 2012) is achieved by multiple E3 ligases; therefore, it is not surprising that budding yeast has evolved multiple mechanisms to counteract the detrimental consequences of overexpressed Cse4 on genome stability. For example, multiple E3 ligases and proteins encoded by *PSH1*, *SLX5*, *RCY1*, and *SPT16* prevent mislocalization of overexpressed Cse4 with only marginal effects when Cse4 is expressed from its own promoter (Ranjitkar *et al.* 2010; Au *et al.* 2013; Deyter and Biggins 2014; Ohkuni *et al.* 2014, 2016; Cheng *et al.* 2016; Hildebrand and Biggins 2016). Here, we define a novel role for the HIR complex in preventing mislocalization of overexpressed Cse4 by facilitating the interaction of Cse4 with Psh1: reduced interaction of Psh1 with Cse4 in *hir2Δ* strains; overlapping peaks of mislocalized Cse4 in *hir2Δ* and *psh1Δ* strains; and, suppression of *GALCSE4* SDL and Cse4 proteolysis defects in *hir2Δ* strains by overexpression of *PSH1*. A recent study has shown that Spt16, a component of the FACT complex, facilitates the activity of Psh1 toward Cse4 (Deyter and Biggins 2014). Interestingly, both *SPT16* and *POB3* exhibit negative genetic interaction with *HIR* (Formosa *et al.* 2002) suggesting that FACT and HIR likely function in separate pathways.

While compromised Psh1-mediated proteolysis contributes in part to the increased stability of Cse4 in *hir2Δ* strains, several lines of evidence support additional, Psh1-independent roles for Hir2 in Cse4 proteolysis. As mentioned above, deletion of Cac2, a component of CAF-1, reduces the deposition of Cse4 into chromatin in a *psh1Δ* mutant and suppresses the SDL phenotype of a *psh1Δ GALCSE4* strain (Hewawasam *et al.* 2018); however, deletion of Cac2 does not suppress the SDL of *hir2Δ GALCSE4* or mislocalization of Cse4 in a *hir2Δ* strain. Second, overexpression of *UBI4* can suppress the SDL of *psh1Δ GALCSE4* as we previously reported (Au *et al.* 2013; Figure S5), but overexpression of *UBI4* does not suppress the SDL of *hir2Δ GALCSE4* and *hir2Δ psh1Δ GALCSE4* strains (Figure S5). Third, protein stability assays show that Cse4 is more stable in the *hir2Δ* strain as compared to the *psh1Δ* strain.

In summary, our genome-wide screen has identified evolutionarily conserved pathways that regulate cellular levels of Cse4 and prevent its mislocalization. We have defined a novel role for the HIR complex in facilitating proteolysis of Cse4, preventing Cse4 mislocalization to noncentromeric regions, and promoting genome stability. The role of the HIR complex in preventing Cse4 mislocalization may be evolutionarily conserved, as knockdown of HIRA shows mislocalization of

CENP-A in human cells (Lacoste *et al.* 2014). Identification of pathways that regulate the proteolysis of overexpressed Cse4 is important from a clinical standpoint because CENP-A is overexpressed and mislocalized in many types of cancers exhibiting aneuploidy (Tomonaga *et al.* 2003; Amato *et al.* 2009; Hu *et al.* 2010; Y. Li *et al.* 2011; Wu *et al.* 2012; Lacoste *et al.* 2014; Athwal *et al.* 2015). Furthermore, overexpression and mislocalization of Cse4, Cnp1, Cid and CENP-A contribute to chromosomal instability in budding yeast, fission yeast, flies, and human cells, respectively (Heun *et al.* 2006; Au *et al.* 2008; Mishra *et al.* 2011; Gonzalez *et al.* 2014; Shrestha *et al.* 2017). Mechanistic insights from regulators of Cse4 in budding yeast and their human homologs will help us better understand how overexpression and mislocalization of CENP-A contribute to tumorigenesis.

Acknowledgments

We are grateful to the members of the Basrai laboratory for helpful discussions and comments on the manuscript. We gratefully acknowledge Sue Biggins for reagents and advice and Kathy McKinnon of the National Cancer Institute Vaccine Branch fluorescence-activated cell sorting (FACS) Core for assistance with FACS analysis. M.A.B. and P.S.M. are supported by the National Institutes of Health (NIH) Intramural Research Program at the National Cancer Institute and D.L. by the NIH Intramural Research Program at the National Library of Medicine. This research was also supported by grants from the NIH to C.L.M. (R01HG005084), to C.B. and C.L.M. (R01HG005853) and to C.B. and M.C. (R01HG005853), from the Canadian Institute of Health Research to C.B. and M.C. (FDN-143264) and the Lewis-Sigler Fellowship to A.B. C.L.M. and C.B. are fellows in the Canadian Institute for Advanced Research (CIFAR, https://www.cifar.ca/) Genetic Networks Program. The funders had no role in study design, data collection and analysis, decision to publish, or preparation of the manuscript.

Literature Cited

Allshire, R. C., and G. H. Karpen, 2008 Epigenetic regulation of centromeric chromatin: old dogs, new tricks? Nat. Rev. Genet. 9: 923–937. https://doi.org/10.1038/nrg2466

Amato, A., T. Schillaci, L. Lentini, and A. Di Leonardo, 2009 CENPA overexpression promotes genome instability in pRb-depleted human cells. Mol. Cancer 8: 119. https://doi.org/10.1186/1476-4598-8-119

Amin, A. D., N. Vishnoi, and P. Prochasson, 2013 A global requirement for the HIR complex in the assembly of chromatin. Biochim. Biophys. Acta 1819: 264–276. https://doi.org/10.1016/j.bbagrm.2011.07.008

Athwal, R. K., M. P. Walkiewicz, S. Baek, S. Fu, M. Bui *et al.*, 2015 CENP-A nucleosomes localize to transcription factor hotspots and subtelomeric sites in human cancer cells. Epigenetics Chromatin 8: 2. https://doi.org/10.1186/1756-8935-8-2

Au, W. C., M. J. Crisp, S. Z. DeLuca, O. J. Rando, and M. A. Basrai, 2008 Altered dosage and mislocalization of histone H3 and Cse4p lead to chromosome loss in Saccharomyces cerevisiae. Genetics 179: 263–275. https://doi.org/10.1534/genetics.108.088518

Au, W. C., A. R. Dawson, D. W. Rawson, S. B. Taylor, R. E. Baker *et al.*, 2013 A novel role of the N-terminus of budding yeast histone H3 variant Cse4 in ubiquitin-mediated proteolysis. Genetics 194: 513–518. https://doi.org/10.1534/genetics.113.149898

Baryshnikova, A., M. Costanzo, S. Dixon, F. J. Vizeacoumar, C. L. Myers *et al.*, 2010a Synthetic genetic array (SGA) analysis in Saccharomyces cerevisiae and Schizosaccharomyces pombe. Methods Enzymol. 470: 145–179. https://doi.org/10.1016/S0076-6879(10)70007-0

Baryshnikova, A., M. Costanzo, Y. Kim, H. Ding, J. Koh *et al.*, 2010b Quantitative analysis of fitness and genetic interactions in yeast on a genome scale. Nat. Methods 7: 1017–1024. https://doi.org/10.1038/nmeth.1534

Bortvin, A., and F. Winston, 1996 Evidence that Spt6p controls chromatin structure by a direct interaction with histones. Science 272: 1473–1476. https://doi.org/10.1126/science.272.5267.1473

Burrack, L. S., and J. Berman, 2012 Flexibility of centromere and kinetochore structures. Trends Genet. 28: 204–212. https://doi.org/10.1016/j.tig.2012.02.003

Canzonetta, C., S. Vernarecci, M. Iuliani, C. Marracino, C. Belloni *et al.*, 2015 SAGA DUB-Ubp8 deubiquitylates centromeric histone variant Cse4. G3 (Bethesda) 6: 287–298. https://doi.org/10.1534/g3.115.024877

Castillo, A. G., A. L. Pidoux, S. Catania, M. Durand-Dubief, E. S. Choi *et al.*, 2013 Telomeric repeats facilitate CENP-A(Cnp1) incorporation via telomere binding proteins. PLoS One 8: e69673. https://doi.org/10.1371/journal.pone.0069673

Chen, Y., R. E. Baker, K. C. Keith, K. Harris, S. Stoler *et al.*, 2000 The N terminus of the centromere H3-like protein Cse4p performs an essential function distinct from that of the histone fold domain. Mol. Cell. Biol. 20: 7037–7048. https://doi.org/10.1128/MCB.20.18.7037-7048.2000

Cheng, H., X. Bao, and H. Rao, 2016 The F-box protein Rcy1 is involved in the degradation of histone H3 variant Cse4 and genome maintenance. J. Biol. Chem. 291: 10372–10377. https://doi.org/10.1074/jbc.M115.701813

Cheng, H., X. Bao, X. Gan, S. Luo, and H. Rao, 2017 Multiple E3s promote the degradation of histone H3 variant Cse4. Sci. Rep. 7: 8565. https://doi.org/10.1038/s41598-017-08923-w

Choi, E. S., A. Stralfors, S. Catania, A. G. Castillo, J. P. Svensson *et al.*, 2012 Factors that promote H3 chromatin integrity during transcription prevent promiscuous deposition of CENP-A (Cnp1) in fission yeast. PLoS Genet. 8: e1002985. https://doi.org/10.1371/journal.pgen.1002985

Choy, J. S., P. K. Mishra, W. C. Au, and M. A. Basrai, 2012 Insights into assembly and regulation of centromeric chromatin in Saccharomyces cerevisiae. Biochim. Biophys. Acta 1819: 776–783. https://doi.org/10.1016/j.bbagrm.2012.02.008

Clarke, L., and J. Carbon, 1980 Isolation of a yeast centromere and construction of functional small circular chromosomes. Nature 287: 504–509. https://doi.org/10.1038/287504a0

Collins, K. A., S. Furuyama, and S. Biggins, 2004 Proteolysis contributes to the exclusive centromere localization of the yeast Cse4/CENP-A histone H3 variant. Curr. Biol. 14: 1968–1972. https://doi.org/10.1016/j.cub.2004.10.024

Collins, K. A., A. R. Castillo, S. Y. Tatsutani, and S. Biggins, 2005 De novo kinetochore assembly requires the centromeric histone H3 variant. Mol. Biol. Cell 16: 5649–5660. https://doi.org/10.1091/mbc.e05-08-0771

Costanzo, M., A. Baryshnikova, J. Bellay, Y. Kim, E. D. Spear *et al.*, 2010 The genetic landscape of a cell. Science 327: 425–431. https://doi.org/10.1126/science.1180823

Costanzo, M., B. VanderSluis, E. N. Koch, A. Baryshnikova, C. Pons *et al.*, 2016 A global genetic interaction network maps a wiring diagram of cellular function. Science 353: pii: aaf1420.

Crotti, L. B., and M. A. Basrai, 2004 Functional roles for evolutionarily conserved Spt4p at centromeres and heterochromatin

in Saccharomyces cerevisiae. EMBO J. 23: 1804–1814. https://doi.org/10.1038/sj.emboj.7600161

DeSilva, H., K. Lee, and M. A. Osley, 1998 Functional dissection of yeast Hir1p, a WD repeat-containing transcriptional corepressor. Genetics 148: 657–667.

Deyter, G. M., and S. Biggins, 2014 The FACT complex interacts with the E3 ubiquitin ligase Psh1 to prevent ectopic localization of CENP-A. Genes Dev. 28: 1815–1826. https://doi.org/10.1101/gad.243113.114

Deyter, G. M., E. M. Hildebrand, A. D. Barber, and S. Biggins, 2017 Histone H4 facilitates the proteolysis of the budding yeast CENP-ACse4 centromeric histone variant. Genetics 205: 113–124. https://doi.org/10.1534/genetics.116.194027

Ferreira, M. E., K. Flaherty, and P. Prochasson, 2011 The Saccharomyces cerevisiae histone chaperone Rtt106 mediates the cell cycle recruitment of SWI/SNF and RSC to the HIR-dependent histone genes. PLoS One 6: e21113. https://doi.org/10.1371/journal.pone.0021113

Fillingham, J., P. Kainth, J. P. Lambert, H. van Bakel, K. Tsui *et al.*, 2009 Two-color cell array screen reveals interdependent roles for histone chaperones and a chromatin boundary regulator in histone gene repression. Mol. Cell 35: 340–351. https://doi.org/10.1016/j.molcel.2009.06.023

Formosa, T., S. Ruone, M. D. Adams, A. E. Olsen, P. Eriksson *et al.*, 2002 Defects in SPT16 or POB3 (yFACT) in Saccharomyces cerevisiae cause dependence on the Hir/Hpc pathway: polymerase passage may degrade chromatin structure. Genetics 162: 1557–1571.

Gentleman, R. C., V. J. Carey, D. M. Bates, B. Bolstad, M. Dettling *et al.*, 2004 Bioconductor: open software development for computational biology and bioinformatics. Genome Biol. 5: R80. https://doi.org/10.1186/gb-2004-5-10-r80

Gonzalez, M., H. He, Q. Dong, S. Sun, and F. Li, 2014 Ectopic centromere nucleation by CENP–a in fission yeast. Genetics 198: 1433–1446. https://doi.org/10.1534/genetics.114.171173

Green, E. M., A. J. Antczak, A. O. Bailey, A. A. Franco, K. J. Wu *et al.*, 2005 Replication-independent histone deposition by the HIR complex and Asf1. Curr. Biol. 15: 2044–2049. https://doi.org/10.1016/j.cub.2005.10.053

Grøntved, L., J. J. Waterfall, D. W. Kim, S. Baek, M. H. Sung *et al.*, 2015 Transcriptional activation by the thyroid hormone receptor through ligand-dependent receptor recruitment and chromatin remodelling. Nat. Commun. 6: 7048. https://doi.org/10.1038/ncomms8048

Gunjan, A., J. Paik, and A. Verreault, 2005 Regulation of histone synthesis and nucleosome assembly. Biochimie 87: 625–635. https://doi.org/10.1016/j.biochi.2005.02.008

Henikoff, S., 2012 Chromatin processes, epigenetic inheritance, centromere structure and function and evolution. Curr. Biol. 22: R106–R107. https://doi.org/10.1016/j.cub.2011.12.014

Herrero, E., and P. H. Thorpe, 2016 Synergistic control of kinetochore protein levels by Psh1 and Ubr2. PLoS Genet. 12: e1005855. https://doi.org/10.1371/journal.pgen.1005855

Heun, P., S. Erhardt, M. D. Blower, S. Weiss, A. D. Skora *et al.*, 2006 Mislocalization of the Drosophila centromere-specific histone CID promotes formation of functional ectopic kinetochores. Dev. Cell 10: 303–315. https://doi.org/10.1016/j.devcel.2006.01.014

Hewawasam, G., M. Shivaraju, M. Mattingly, S. Venkatesh, S. Martin-Brown *et al.*, 2010 Psh1 is an E3 ubiquitin ligase that targets the centromeric histone variant Cse4. Mol. Cell 40: 444–454. https://doi.org/10.1016/j.molcel.2010.10.014

Hewawasam, G. S., M. Mattingly, S. Venkatesh, Y. Zhang, L. Florens *et al.*, 2014 Phosphorylation by casein kinase 2 facilitates Psh1 protein-assisted degradation of Cse4 protein. J. Biol. Chem. 289: 29297–29309. https://doi.org/10.1074/jbc.M114.580589

Hewawasam, G. S., K. Dhatchinamoorthy, M. Mattingly, C. Seidel, and J. L. Gerton, 2018 Chromatin assembly factor-1 (CAF-1) chaperone regulates Cse4 deposition into chromatin in budding yeast. Nucleic Acids Res. 46: 4440–4455. https://doi.org/10.1093/nar/gky405

Hildebrand, E. M., and S. Biggins, 2016 Regulation of budding yeast CENP-A levels prevents misincorporation at promoter nucleosomes and transcriptional defects. PLoS Genet. 12: e1005930. https://doi.org/10.1371/journal.pgen.1005930

Hornung, P., P. Troc, F. Malvezzi, M. Maier, Z. Demianova *et al.*, 2014 A cooperative mechanism drives budding yeast kinetochore assembly downstream of CENP-A. J. Cell Biol. 206: 509–524. https://doi.org/10.1083/jcb.201403081

Hu, Z., G. Huang, A. Sadanandam, S. Gu, M. E. Lenburg *et al.*, 2010 The expression level of HJURP has an independent prognostic impact and predicts the sensitivity to radiotherapy in breast cancer. Breast Cancer Res. 12: R18. https://doi.org/10.1186/bcr2487

Kastenmayer, J. P., L. Ni, A. Chu, L. E. Kitchen, W. C. Au *et al.*, 2006 Functional genomics of genes with small open reading frames (sORFs) in S. cerevisiae. Genome Res. 16: 365–373. https://doi.org/10.1101/gr.4355406

Lacoste, N., A. Woolfe, H. Tachiwana, A. V. Garea, T. Barth *et al.*, 2014 Mislocalization of the centromeric histone variant CenH3/CENP-A in human cells depends on the chaperone DAXX. Mol. Cell 53: 631–644. https://doi.org/10.1016/j.molcel.2014.01.018

Li, Y., Z. Zhu, S. Zhang, D. Yu, H. Yu *et al.*, 2011 ShRNA-targeted centromere protein A inhibits hepatocellular carcinoma growth. PLoS One 6: e17794. https://doi.org/10.1371/journal.pone.0017794

Li, Z., F. J. Vizeacoumar, S. Bahr, J. Li, J. Warringer *et al.*, 2011 Systematic exploration of essential yeast gene function with temperature-sensitive mutants. Nat. Biotechnol. 29: 361–367. https://doi.org/10.1038/nbt.1832

Livak, K. J., and T. D. Schmittgen, 2001 Analysis of relative gene expression data using real-time quantitative PCR and the 2(-Delta C(T)). Method. Methods 25: 402–408. https://doi.org/10.1006/meth.2001.1262

Longtine, M. S., A. McKenzie, III, D. J. Demarini, N. G. Shah, A. Wach *et al.*, 1998 Additional modules for versatile and economical PCR-based gene deletion and modification in Saccharomyces cerevisiae. Yeast 14: 953–961. https://doi.org/10.1002/(SICI)1097-0061(199807)14:10<953::AID-YEA293>3.0.CO;2-U

Lopes da Rosa, J., J. Holik, E. M. Green, O. J. Rando, and P. D. Kaufman, 2011 Overlapping regulation of CenH3 localization and histone H3 turnover by CAF-1 and HIR proteins in Saccharomyces cerevisiae. Genetics 187: 9–19. https://doi.org/10.1534/genetics.110.123117

Love, I. M., and S. R. Grossman, 2012 It takes 15 to tango: making sense of the many ubiquitin ligases of p53. Genes Cancer 3: 249–263. https://doi.org/10.1177/1947601912455198

Lycan, D. E., M. A. Osley, and L. M. Hereford, 1987 Role of transcriptional and posttranscriptional regulation in expression of histone genes in Saccharomyces cerevisiae. Mol. Cell. Biol. 7: 614–621. https://doi.org/10.1128/MCB.7.2.614

Maddox, P. S., K. D. Corbett, and A. Desai, 2012 Structure, assembly and reading of centromeric chromatin. Curr. Opin. Genet. Dev. 22: 139–147. https://doi.org/10.1016/j.gde.2011.11.005

McKinley, K. L., and I. M. Cheeseman, 2016 The molecular basis for centromere identity and function. Nat. Rev. Mol. Cell Biol. 17: 16–29. https://doi.org/10.1038/nrm.2015.5

Metzger, M. B., J. L. Scales, M. F. Dunklebarger, and A. M. Weissman, 2017 The ubiquitin ligase (E3) Psh1p is required for proper segregation of both centromeric and two-micron plasmids in

Saccharomyces cerevisiae. G3 (Bethesda) 7: 3731–3743. https://doi.org/10.1534/g3.117.300227
Mishra, P. K., M. Baum, and J. Carbon, 2007 Centromere size and position in Candida albicans are evolutionarily conserved independent of DNA sequence heterogeneity. Mol. Genet. Genomics 278: 455–465. https://doi.org/10.1007/s00438-007-0263-8
Mishra, P. K., W. C. Au, J. S. Choy, P. H. Kuich, R. E. Baker *et al.*, 2011 Misregulation of Scm3p/HJURP causes chromosome instability in Saccharomyces cerevisiae and human cells. PLoS Genet. 7: e1002303. https://doi.org/10.1371/journal.pgen.1002303
Mishra, P. K., S. Ciftci-Yilmaz, D. Reynolds, W. C. Au, L. Boeckmann *et al.*, 2016 Polo kinase Cdc5 associates with centromeres to facilitate the removal of centromeric cohesin during mitosis. Mol. Biol. Cell 27: 2286–2300. https://doi.org/10.1091/mbc.e16-01-0004
Mishra, P. K., K. S. Thapa, P. Chen, S. Wang, T. R. Hazbun *et al.*, 2018 Budding yeast CENP-A(Cse4) interacts with the N-terminus of Sgo1 and regulates its association with centromeric chromatin. Cell Cycle 17: 11–23. https://doi.org/10.1080/15384101.2017.1380129
Moreno-Moreno, O., S. Medina-Giro, M. Torras-Llort, and F. Azorin, 2011 The F box protein partner of paired regulates stability of Drosophila centromeric histone H3, CenH3(CID). Curr. Biol. 21: 1488–1493. https://doi.org/10.1016/j.cub.2011.07.041
Morey, L., K. Barnes, Y. Chen, M. Fitzgerald-Hayes, and R. E. Baker, 2004 The histone fold domain of Cse4 is sufficient for CEN targeting and propagation of active centromeres in budding yeast. Eukaryot. Cell 3: 1533–1543. https://doi.org/10.1128/EC.3.6.1533-1543.2004
Ohkuni, K., R. Abdulle, and K. Kitagawa, 2014 Degradation of centromeric histone H3 variant Cse4 requires the Fpr3 peptidyl-prolyl Cis-Trans isomerase. Genetics 196: 1041–1045. https://doi.org/10.1534/genetics.114.161224
Ohkuni, K., Y. Takahashi, A. Fulp, J. Lawrimore, W. C. Au *et al.*, 2016 SUMO-targeted ubiquitin ligase (STUbL) Slx5 regulates proteolysis of centromeric histone H3 variant Cse4 and prevents its mislocalization to euchromatin. Mol. Biol. Cell 27: 1500–1510. https://doi.org/10.1091/mbc.e15-12-0827
Ortiz, J., O. Stemmann, S. Rank, and J. Lechner, 1999 A putative protein complex consisting of Ctf19, Mcm21, and Okp1 represents a missing link in the budding yeast kinetochore. Genes Dev. 13: 1140–1155. https://doi.org/10.1101/gad.13.9.1140
Osley, M. A., 1991 The regulation of histone synthesis in the cell cycle. Annu. Rev. Biochem. 60: 827–861. https://doi.org/10.1146/annurev.bi.60.070191.004143
Osley, M. A., and D. Lycan, 1987 Trans-acting regulatory mutations that alter transcription of Saccharomyces cerevisiae histone genes. Mol. Cell. Biol. 7: 4204–4210. https://doi.org/10.1128/MCB.7.12.4204
Osley, M. A., J. Gould, S. Kim, M. Y. Kane, and L. Hereford, 1986 Identification of sequences in a yeast histone promoter involved in periodic transcription. Cell 45: 537–544. https://doi.org/10.1016/0092-8674(86)90285-0
Przewloka, M. R., and D. M. Glover, 2009 The kinetochore and the centromere: a working long distance relationship. Annu. Rev. Genet. 43: 439–465. https://doi.org/10.1146/annurev-genet-102108-134310
Ranjitkar, P., M. O. Press, X. Yi, R. Baker, M. J. MacCoss *et al.*, 2010 An E3 ubiquitin ligase prevents ectopic localization of the centromeric histone H3 variant via the centromere targeting domain. Mol. Cell 40: 455–464. https://doi.org/10.1016/j.molcel.2010.09.025
Robinson, J. T., H. Thorvaldsdottir, W. Winckler, M. Guttman, E. S. Lander *et al.*, 2011 Integrative genomics viewer. Nat. Biotechnol. 29: 24–26. https://doi.org/10.1038/nbt.1754
Schneider, C. A., W. S. Rasband, and K. W. Eliceiri, 2012 NIH Image to ImageJ: 25 years of image analysis. Nat. Methods 9: 671–675. https://doi.org/10.1038/nmeth.2089
Seoighe, C., and K. H. Wolfe, 1999 Updated map of duplicated regions in the yeast genome. Gene 238: 253–261. https://doi.org/10.1016/S0378-1119(99)00319-4
Shrestha, R. L., G. S. Ahn, M. I. Staples, K. M. Sathyan, T. S. Karpova *et al.*, 2017 Mislocalization of centromeric histone H3 variant CENP-A contributes to chromosomal instability (CIN) in human cells. Oncotarget 8: 46781–46800. https://doi.org/10.18632/oncotarget.18108
Silva, A. C., X. Xu, H. S. Kim, J. Fillingham, T. Kislinger *et al.*, 2012 The replication-independent histone H3–H4 chaperones HIR, ASF1, and RTT106 co-operate to maintain promoter fidelity. J. Biol. Chem. 287: 1709–1718. https://doi.org/10.1074/jbc.M111.316489
Singh, R. K., M. Gonzalez, M. H. Kabbaj, and A. Gunjan, 2012 Novel E3 ubiquitin ligases that regulate histone protein levels in the budding yeast Saccharomyces cerevisiae. PLoS One 7: e36295. https://doi.org/10.1371/journal.pone.0036295
Spector, M. S., A. Raff, H. DeSilva, K. Lee, and M. A. Osley, 1997 Hir1p and Hir2p function as transcriptional corepressors to regulate histone gene transcription in the Saccharomyces cerevisiae cell cycle. Mol. Cell. Biol. 17: 545–552. https://doi.org/10.1128/MCB.17.2.545
Tomonaga, T., K. Matsushita, S. Yamaguchi, T. Oohashi, H. Shimada *et al.*, 2003 Overexpression and mistargeting of centromere protein-A in human primary colorectal cancer. Cancer Res. 63: 3511–3516.
Tong, A. H., G. Lesage, G. D. Bader, H. Ding, H. Xu *et al.*, 2004 Global mapping of the yeast genetic interaction network. Science 303: 808–813. https://doi.org/10.1126/science.1091317
Usaj, M., Y. Tan, W. Wang, B. VanderSluis, A. Zou *et al.*, 2017 TheCellMap.org: a web-accessible database for visualizing and mining the global yeast genetic interaction network. G3 (Bethesda) 7: 1539–1549. https://doi.org/10.1534/g3.117.040220
Verdaasdonk, J. S., and K. Bloom, 2011 Centromeres: unique chromatin structures that drive chromosome segregation. Nat. Rev. Mol. Cell Biol. 12: 320–332. https://doi.org/10.1038/nrm3107
Wieland, G., S. Orthaus, S. Ohndorf, S. Diekmann, and P. Hemmerich, 2004 Functional complementation of human centromere protein A (CENP-A) by Cse4p from Saccharomyces cerevisiae. Mol. Cell. Biol. 24: 6620–6630. https://doi.org/10.1128/MCB.24.15.6620-6630.2004
Wu, Q., Y. M. Qian, X. L. Zhao, S. M. Wang, X. J. Feng *et al.*, 2012 Expression and prognostic significance of centromere protein A in human lung adenocarcinoma. Lung Cancer 77: 407–414. https://doi.org/10.1016/j.lungcan.2012.04.007
Xu, H., U. J. Kim, T. Schuster, and M. Grunstein, 1992 Identification of a new set of cell cycle-regulatory genes that regulate S-phase transcription of histone genes in Saccharomyces cerevisiae. Mol. Cell. Biol. 12: 5249–5259. https://doi.org/10.1128/MCB.12.11.5249
Zang, C., D. E. Schones, C. Zeng, K. Cui, K. Zhao *et al.*, 2009 A clustering approach for identification of enriched domains from histone modification ChIP-Seq data. Bioinformatics 25: 1952–1958. https://doi.org/10.1093/bioinformatics/btp340

Communicating editor: S. Biggins